Multi-agent MPC protocols for micro-grid energy management and optimization

Multiagentní MPC protokoly pro energetickou optimalizaci mikrosítě

Pavel Elis

Master Thesis

T.I.M.E. Double Degree

MASTER'S THESIS ASSIGNMENT

I. Personal and study details

Student's name:	**Elis Pavel**	Personal ID number:	**420232**
Faculty / Institute:	**Faculty of Electrical Engineering**		
Department / Institute:	**Department of Control Engineering**		
Study program:	**Cybernetics and Robotics**		
Branch of study:	**Cybernetics and Robotics**		

II. Master's thesis details

Master's thesis title in English:

Multi-agent MPC protocols for microgrid energy management and optimization

Master's thesis title in Czech:

Multiagentní MPC protokoly pro energetickou optimalizaci mikrosítě

Guidelines:

1. Describe the current state-of-the-art, detailing the existing control strategies for microgrids [1] [2].
2. Describe and analyse the given (situation on the) demonstration site and assess the possible optimization approaches utilizing multi-agent systems, [3] [4].
3. Structure the available test data and identify appropriate evaluation metrics, [1].
4. Design a multi-agent MPC protocol for the demonstration site; validate and evaluate the results, [5].

Bibliography / sources:

[1] G. Gürses-Tran, D. Mildt, M. Hirst, M. Cupelli, A. Monti, "MPC based energy management optimization for a European microgrid implementation", 2019, 25th International Conference on Electricity Distribution, Madrid
(wasn't published yet)
[2] A. Ulbig and G. Andersson, "Analyzing operational flexibility of electric power systems," 2014 Power Systems Computation Conference, Wroclaw, 2014, pp. 1-8.
[3] T. L. Nguyen, Q. Tran, R. Caire, C. Gavriluta and V. H. Nguyen, "Agent based distributed control of islanded microgrid — Real-time cyber-physical implementation," 2017 IEEE PES Innovative Smart Grid Technologies Conference Europe (ISGT-Europe), Torino, 2017, pp. 1-6.
[4] M. Reyasudin Basir Khan, Razali Jidin, Jagadeesh Pasupuleti "Multi-agent based distributed control architecture for microgrid energy management and optimization" 2016 Energy Conversion and Management, College of Engineering, Universiti Tenaga Nasional, Jalan IKRAM – UNITEN, 43000 Kajang, Selangor, Malaysia
[5] D. Mildt, M. Cupelli, A. Monti, "Objective Trade-off in MPC based Based Energy Management for Microgrids",
(wasn't published yet)

Name and workplace of master's thesis supervisor:

Kristian Hengster-Movric, Ph.D., Department of Control Engineering, FEE

Name and workplace of second master's thesis supervisor or consultant:

Date of master's thesis assignment: **13.02.2019**   Deadline for master's thesis submission: _____

Assignment valid until:
by the end of summer semester 2019/2020

Kristian Hengster-Movric, Ph.D.	prof. Ing. Michael Šebek, DrSc.	prof. Ing. Pavel Ripka, CSc.
Supervisor's signature	Head of department's signature	Dean's signature

III. Assignment receipt

The student acknowledges that the master's thesis is an individual work. The student must produce his thesis without the assistance of others, with the exception of provided consultations. Within the master's thesis, the author must state the names of consultants and include a list of references.

15. 4. 2019
_____
Date of assignment receipt

_____
Student's signature

Declaration

I declare that the presented work was developed independently and that I have listed all sources of information used within it in accordance with the methodical instructions for observing the ethical principles in the preparation of university theses.

————————————————————   ————————————————————
Place, Date   Signature

Prohlášení autora práce

Prohlašuji, že jsem předloženou práci vypracoval samostatně a že jsem uvedl veškeré použité informační zdroje v souladu s Metodickým pokynem o dodržování etických principů při přípravě vysokoškolských závěrečných prací.

————————————————————   ————————————————————
Místo, Datum   Podpis

Acknowledgement

I would like to express my appreciation to both of my supervisors, Kristian Hengster-Movric, Ph.D. and M.Sc. Gonca Gürses-Tran, for their guidance and valuable advice during the whole process of my master thesis. Moreover, I would like to thank my parents for their mental and financial support during my studies abroad.

Abstract

One of the challenges of microgrids under the influence of high shares of intermittent renewable energy sources (RES) is an effective and reliable control. Model predictive control (MPC) is a promising approach to solve this problem for a specified time horizon since it allows integrating of a cost-minimizing objective function and system boundaries while taking power demand and supply into account.

An agent-based MPC scheme was developed as a two-level architecture based on multi-agent control system (MAS) consensus algorithm providing power balance in the microgrid and centralized MPC that is aspiring to streamline the control processes to reach the targeted objectives.

During the examination of the simulated results, the expected correlation of the result properties and control parameters was found. Additionally, the situations with the highest improvement ratio in comparison with the results of the reference control architecture were discovered and analysed.

Based on the results, a significant cost reduction can be seen in most of the tested datasets that were measured on a real-life microgrid solution. Therefore, the implementation of the suggested control can prove to be appropriate and beneficial for microgrid operators and grid customers.

Keywords: Power system, Microgrid, Multi-agent control, MPC, Consensus

Abstrakt

Navržení efektivního a spolehlivého řízení mikrosítí s vysokým podílem energie z obnovitelných zdrojů, je jednou z výzev při jejich nasazení. Prediktivní řízení (MPC) systému je slibný přístup, jak vyřešit tento problém v určitém časovém horizontu. Tento přístup umožňuje integraci řízení na základě minimalizace funkce, která dává do souvislosti různé druhy nákladů a omezení systému, ve vazbě na výrobu a spotřebu energie.

Navržené multiagentní MPC řízení bylo vyvinuto jako dvoustupňová architektura, založená na konsensuálním algoritmu více agentů, který zajišťuje výkonovou rovnováhu v mikrosíti a centralizovaném MPC, který zefektivňuje řízené procesy tak, aby dosáhly vytyčených cílů.

Při zkoumání navržených simulací byla ověřena předpokládaná korelace získaných výsledků a řídicích parametrů. Dále byla identifikována a analyzována situace s nejvyšším zlepšením ve srovnání s výsledky referenční řídící architektury.

Na základě výsledků testů řídicího protokolu na testovaných datech, které byly měřeny v reálné mikrosíti, je vidět možnost významného snížení nákladů na provoz mikrosítě. Navrhované řešení tedy ukazuje vhodnost jeho implementace a přínos, jak pro provozovatele mikrosítí, tak pro zákazníky distribuční soustavy.

Klíčová slova: Energetický systém, Mikrosíť, Multiagentní řízení, MPC, Konsensus

Contents

Contents

Acronyms

CO_2 Carbon Dioxide 5, 9, 10

A/C Air-condition 13

AC Alternating Current 7, 9, 11, 15, 17, 31

BESS Battery Energy Storage System xii, 8, 10, 11, 14, 18, 19, 31, 34, 35, 37–40, 42, 44, 46–48, 51–61, 63, 64, 71, 73

BUG Back-up Generator 9, 10, 31, 34, 38, 42–44, 48

CCHP Combined Cooling, Heating And Power System 14, 15

CCVSI Current-controlled Voltage Source Inverters 17, 18

CT Current Transformer 8

DC Direct Current 7, 9, 11, 15, 16, 31

DER Distributed Energy Resources 6, 15

DG Distributed Generation 5

DSM Demand Side Management 12

EMS Energy Management System 6, 8, 15

ESS Energy Storage System 7, 10, 15–20, 53, 54

EU European Union 6

HESS Hybrid Energy Storage System 18

HV High Voltage 11

IEEE The Institute Of Electrical And Electronics Engineers 6, 8

LC Local Controller 16

Li-ion Lithium-ion 54, 64

1

Acronyms

LTI Linear Time-invariant 24, 25

MAS Multi-agent Control System vii, xi, 16, 20, 22, 23, 38, 40–43, 45, 63, 73

MMSE Minimized Mean Square Error 48

MPC Model Predictive Control vii, 3, 4, 23–25, 37–39, 46–49, 52, 55, 59, 63, 64

MV Medium Voltage 11

OPF Optimal Power Flow Problem 15

PCC Point of Common Coupling 8, 11, 20, 32, 48, 51, 54

PID Proportional–integral–derivative Control 24

PT Potential Transformer 8

PV Photovoltaic 9, 12, 20, 31, 33, 38

QP Quadratic Programming 28

RES Renewable Energy Sources vii, 3, 5, 10

SARIMA Seasonal Autoregressive Integrated Moving Average 48, 49, 54, 63, 71

SMES Superconducting Magnetic Energy Storage System 11

SoC State of Charge 16–19, 34, 37, 38, 42, 46, 47, 52, 56, 64

USA United States of America 5

V2G Vehicle-to-grid 14

VCVSI Voltage-controlled Voltage Source Inverters 17, 18

VPP Virtual Power Plant 15

2

1 Introduction

As a result of the climate change incentives, governments around the world are limiting the number of fossil-fuelled power plants. Similarly, large nuclear power plants are getting less and less popular due to safety concerns and high initial costs. Shutting down of these centrally located high power generators is completely changing the power grid. The energy generation nowadays happens in an increasingly decentralized manner. Such change does not only affect the energy path between the producers and the consumers but also introduces the need to develop novel control architectures [1].

The need to adapt to these challenges motivates the implementation of renewable energy sources (RES) into the grid. However, the operation and control of systems with major RES contribution is more complex and volatile due to their dependence on meteorological inputs. In this context, a major research effort is currently undertaken concerning future reliable and resilient power system operation. Among this, the concept of microgrids and local energy communities emerges, see [2, 3]. This power system structure, based on the separation of a part of the power grid, is able to significantly lower the general complexity of the whole system. Additionally, it provides opportunities for more effective control of the installed renewable sources.

There are a number of possibilities to realize the microgrid control, as for example [4, 5]. Existing solutions differ not only in the implementation of actual algorithms but also in the overall structure of each microgrid. For this reason, microgrid control is often precisely designed to fit the features of a specific system.

Generally, the control of microgrids does not have to differ from the conventional control of power grids. In this case, the well-known three-level control architecture with decentralized primary control and centralized secondary and tertiary control is embedded, [5]. The microgrids, however, bring opportunities for the design of more scalable, reliable and efficient control concepts such as the distributed control. Various distributed cooperative control approaches are presented in numerous articles, see [6, 7, 8, 9].

Model predictive control (MPC), [10, 11, 12], is also widely used for microgrids. It enables to incorporate the knowledge about power generation from renewables over a specific time horizon in the decision-making process. In this way, the controller performance can be improved, especially when the knowledge about the future power generation is subject to low uncertainty, see [13, 14, 15].

In particular, [16, 17, 9] bring a consensus algorithm that provides optimal power resources management based on minimization of quadratic costs of all controllable power resources. However, this particular algorithm, which is often used in the

3

literature fails to converge on arbitrary network topologies even if they contain a spanning tree.

This thesis brings a modified cooperative protocol mitigating the instability issues from [16]. Moreover, the algorithm works on arbitrary communication graph topologies containing a spanning tree. Furthermore, this consensus algorithm is combined with a higher level MPC protocol to achieve optimal dispatch of energy resources.

The dependence of the total algorithm performance on control parameters is identified and the parameters are set so as to optimize the system behaviour according to economical and battery utilization criteria. The developed control architecture is successfully tested on the actual data measured at microgrid *Simris*, deployed as a part of EU project *InterFlex H2020*. The performed tests are very promising; the proposed algorithm outperforms conventional control in most of the tests and brings significant cost reduction when the energy production and consumption of the microgrid are balanced.

In Chapter 2 the concept of microgrids is introduced, followed by the architecture of the typical control strategies for microgrids and the concept of model predictive control. In the second part of the thesis, the implementation of the control algorithm is shown. Chapter 3 describes the scope and objective of the pilot site. Moreover, the underlying dataset and necessary data pre-processing steps are presented. The design of the controller is elaborated in detail in Chapter 4.

In Chapter 5 the simulated results of the implemented control are shown, explained and compared. Conclusions have been drawn in Chapter 6, incorporating the relevance for future work in this field.

2 Microgrid Control Concepts

Due to the rapid population growth and industrialization, the electricity demand is increasing significantly. To cope with this development, the power generation capacity increases accordingly. A major part of the new generation assets (also replacing current bulk power generation) shall be covered by distributed generation (DG) based on RES to achieve lower carbon dioxide (CO_2) emission in the energy sector. Thus, new challenges arise in terms of predicting the grid operating state, since RES are highly intermittent.

As a consequence of population density growth, the energy network will be expanded into very rural places where only the construction of electricity lines for interconnection with the main power grid can become very expensive. Because of the usual low energy demand in these areas, the construction of conventional power plants would not make much sense. Also, covering the demand with central bulk generation is inefficient due to losses and cost of construction of long transmission lines.

One way to solve these problems is the microgrid concept. This idea of grid infrastructure increases the reliability of the network by segmentation which reduces the probability of the black-outs. Therefore, the overall security of supply is increased.

Due to the local distribution of energy resources, the cost of the grid construction can be significantly decreased. The fact, that the energy does not have to travel far, can have a positive influence on the electricity price. The microgrid control, which can lead to the utilization of different energy sources to the economical optimum, can also result in a reduction of the energy price.

In many industrially strong countries, the congestion on the main power lines starts to be a severe problem. The density of the population does not allow the construction of new overhead lines and the upgrade of the existing can be complicated. The dense distribution of power sources and loads (in comparison with today's power system) in microgrids can facilitate the future grid development.

Lastly, smaller systems, such as microgrids, can result in a higher quality of energy supply towards the end consumer, due to a less complex control scheme [18, 19].

2.1 The Microgrid

For a long time, microgrids did not have worldwide-used definition and there are multiple reasons for it. In the different parts of the world, the concept of microgrid was introduced regarding particular motivations.

In the United States of America (USA) the main propagators frequently saw microgrids as the way, how to get electrification to very remote locations and also

how to replace obsolete network infrastructure. In one of the oldest definition of microgrid [20] from 2002, the microgrid is defined as a system which besides electricity provides also heat. The emphasis is placed on the simplicity of connection and disconnection of individual customers, local reliability and security of electricity supply.

On the other hand, in the European Union (EU), the main purpose of microgrid infrastructure is mostly to integrate renewable energy sources and to operate them with maximal efficiency. Due to their intermittent character, they are often used as a negative load in today's network. It is crucial to apply a microgrid control to ensure the efficient utilization of these energy sources and to provide quality, reliable and secure energy supply.

In countries with high dependence on the import of fossil fuels, such as Japan, the microgrid concept can be a technique to reduce their dependence on imported primary energy carriers. This can help to protect the network from frequent energy shortages. For such an innovative country as Japan, this is also a practical approach to test new energy sources and technologies of energy harvesting [18, 21].

The microgrid concept was finally defined in 2017 by *The Institute of Electrical and Electronics Engineers (IEEE) Standard for the Specification of Microgrid Controllers* [22]. By standard *IEEE 2030.7-2017*, a microgrid is a group of interconnected loads and distributed energy resources (DER) with clearly defined electrical boundaries that act as a single controllable entity concerning the grid. It can be connected and disconnected from the grid to operate in grid-connected or islanded modes respectively.

As mentioned in the definition, there are two fundamental modes in which the microgrid can be used.

- **Islanded mode** In the islanded mode the microgrid is disconnected from the macrogrid. During this operation, the energy exchange inside the microgrid is controlled by its central controller.

- **Grid-connected mode** During the operation in the grid-connected mode the microgrid is fully connected to the main macrogrid. The control of the voltage and the frequency level stays in the hands of the macrogrid energy management system (EMS) authorities. The microgrid central controller only coordinate power dispatch of the variable sources and loads to maintain the economical optimization.

The switching between these two modes is done by the locally implemented central controlling system and it does not depend on the macrogrid. The central controller contains the logic that decides if the modes should be changed.

There are many potential reasons to switch between the microgrid's modes. In general, the switching events can be divided into two categories; preplanned and unplanned. In case of preplanned switching event, the incident is scheduled and expected. Therefore, the process of opening/closing of the main switch should lead to minimal transient. Typically, this event occurs during maintenance.

The unplanned switching is usually induced by any type of faults. The way, in which the microgrid controller reacts to this event highly depends on the operating condition before the fault and also on the fault nature. Furthermore, the fault detection interval and microgrid topology influence the final state [23].

Beside distributed generators and distributed loads, the microgrids usually contain energy storage systems (ESSs) that provide the ability to save energy for later use. Energy can be saved not only as an electrical but also in the form of thermal energy or other.

Conventionally, microgrids are designed as separated parts of the main electricity network, thus three-phase alternating current (AC) power systems. Although the biggest advantage of AC systems, easy voltage level change by transformers, is not that crucial for microgrids.

On the other hand, some distributed energy sources are producing direct current (DC) power and that must be later converted by DC/AC converter for connection to the grid. Also, many DC loads use the opposite process to get the power from the grid. Hence, recently fully DC microgrids, as well as hybrid microgrids (partially AC, partially DC), are proposed [24]. Thanks to that, the large power conversion losses can be avoided.
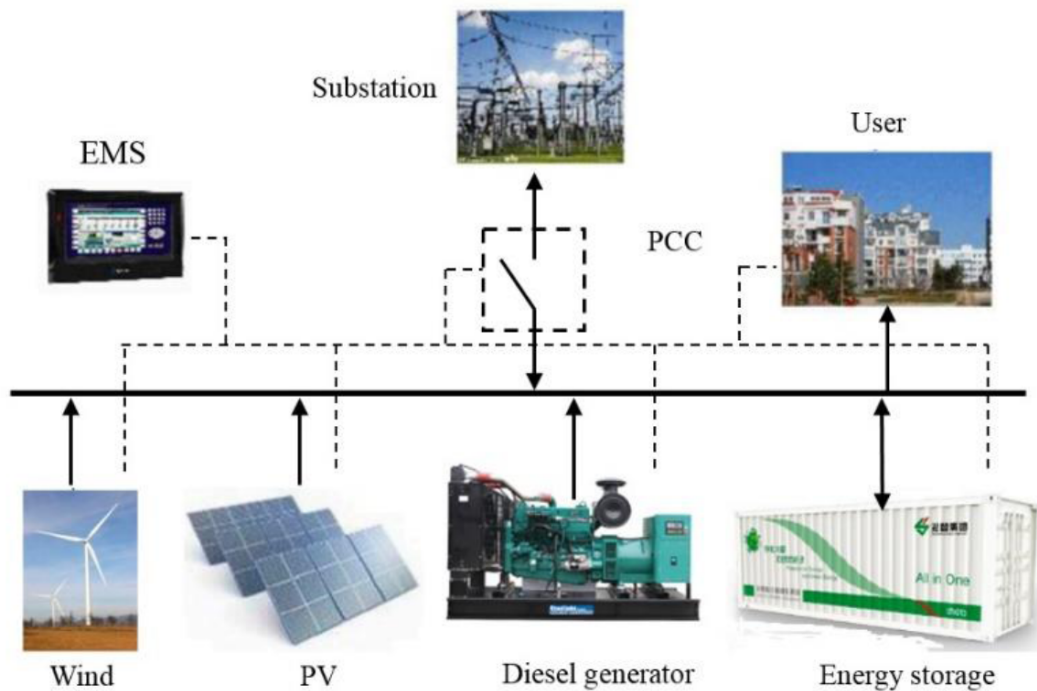

Figure 2.1: Typical microgrid structure [18]

7

In Figure 2.1 the typical structure of a microgrid is visualized. The microgrid is connected to the main grid through substation with main switch (point of common coupling (PCC)). The power flows inside the microgrid and also power exchange with outside are controlled by EMS. Beside that, it consists of energy resources (conventional based on fossil fuels and renewable sources), energy storage (in this case illustrated as BESS inside of container) and final energy users. These components will be discussed in further detail in the following section.

2.1.1 Microgrids components

Typically, microgrids are composed of the following general components. The number of different parts depends on the design of each specific one.

PCC

The main switch connects the microgrid with the macrogrid. This equipment is usually strongly standardized (IEEE 1547) and beside power switching, it also provides power protection, metering, and communication between both sides.

The grid status is measured from both sides of the switch to find out the operating conditions of the microgrid. As it is illustrated in Figure 2.2, the current transformer (CT) and potential transformer (PT) are used for this purpose [25].

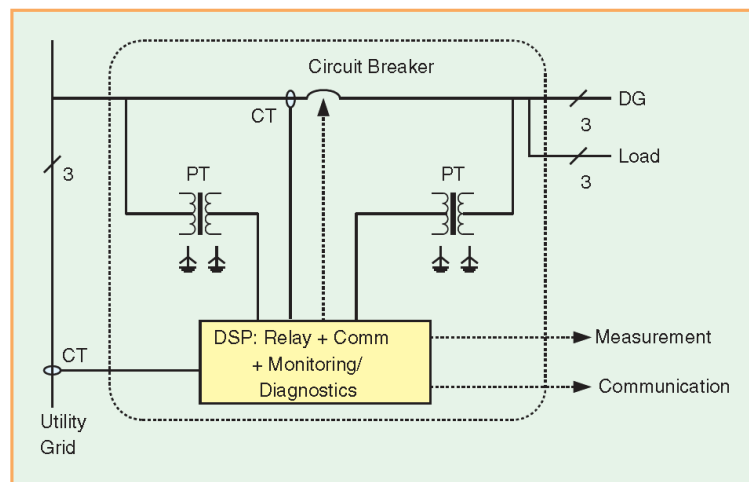Figure 2.2: Schematic diagram of a circuit breaker based interconnection switch [25]

Energy generation

Distributed energy generators are usually small energy sources located near the areas, where the created energy is stored or consumed. Principally we can distinguish between two main types, thermal energy sources that are based on the burning of fossil fuel and renewable energy sources.

The generation of electrical energy can also be combined with other processes such as the usage of thermal energy from waste heat. This process allows us to decrease the overall electricity demand in the microgrid and increase the energy production efficiency significantly.

The energy generators are producing AC or DC power, in case that the microgrid infrastructure is using the other type, the power must be converted by the appropriate power electronics. Many different energy sources are using various ways for electric energy production, only the most fitting ones for microgrids will be listed [23]:

- Combustion engines

- Wind turbines

- Fuel-cells

- Photovoltaic system (or solar-thermal systems)

Typically, the combustion engines transform chemical energy stored in fuel material to mechanical energy by burning process. Even though some renewable fuels exist, most combustion engines run on fossil fuels and usually produce CO_2 emissions. The fuel-burning process can be initialized at any moment and after start-up time the output power of the engine is easy to regulate. Therefore, in microgrid concepts, they are usually used as back-up generators and their usage in the microgrid should be limited.

On the other hand, the energy generation from renewable sources is strongly supported. The wind turbine converts the mechanical energy of the wind to electric energy. They can be designed in many different sizes from small household applications to large wind turbines located in off-shore wind parks with rated power up to 10 MW. The total amount of installed wind turbine capacity is growing worldwide and for many countries and regions, it slowly becomes the most important energy source [26].

Fuel-cell systems convert the chemical energy to electrical not using a burning process as combustion engines but through chemical reaction of hydrogen and oxygen. Although these two elements are energetically demanding during their production, we can consider fuel-cell as a renewable source. Despite the fact, that the process is not very efficient, the use of fuel-cell can be beneficial in some cases due to the low operational cost.

Photovoltaic (PV) systems consist of PV panels that convert solar radiation into electrical energy. PV systems are often accompanied by additional systems utilizing the same primary energy such as solar-thermal systems for heating purposes. The size of the system can differ from household applications (typically PV panels on roof) to large solar parks. Compared to the wind turbine, the disadvantage of PV panels is the necessity to convert the created power from DC to AC. Despite the large progress in power electronics in recent years, the AC/DC conversion has at best an efficiency of 92% [27].

Energy consumption

Energy consumption represents all electrical energy which is converted to the other energy types and used by end-users. In the concept of power system networks, energy consumption corresponds to all nodes that are taking energy from the grid.

Energy consuming objects can be categorized in multiple ways. Typically, to the size of the customer, we can distinguish between industrial, commercial and residential consumers. Since the consumption of residential consumers is quite unpredictable, it makes sense to aggregate them into bigger groups and create larger virtual objects with large consumption and higher predictability rate for control purposes.

In recent years, the possibility of the controllable load of microgrids has been researched. This concept aims to take less critical consumption processes and shift them such that, from a microgrid operators perspective, an optimal load profile is achieved. Thanks to the load shifting the microgrid control can decrease the divergence between load peaks and valleys and thus follow the production curve of RES accordingly. This topic is further discussed in Section 2.1.3.

Energy storages

Distributed energy storages are crucial components of microgrids which balance a power mismatch between energy generation and consumption in the network.

They are improving the microgrid performance in three ways [25]. First of all, they allow energy resources to run on maximum output when grid capacity is limited. In case that RES generate electrical energy in times of low energy demand in the network, distributes energy storages can charge and thus temporarily consume the energy locally. During low energy generation times, for example at nights, the energy can be discharged and provided to the grid customers. This significantly improves the efficiency of renewable sources and helps to reduce CO_2 emission.

As it was said before, the largest disadvantage of many renewable sources is their intermittency. In case of fluctuation of the primary energies of these generators, the distributed energy storages can replace them as a power source.

Lastly, the storages can help during disturbances, maintenance or unplanned outages of the network. The BESSs are systems with very steep starting ramp that makes them usable almost immediately. Therefore, in case of faults, this ESSs can provide energy and support the most important processes before while BUGs are slowly activated.

The different distributed energy storages can store energy in the form of electrical, chemical, mechanical or in other type of energy [23]:

- BESS

- Capacitor/Super-capacitor storage

- Low- and high-speed flywheel

- Superconducting magnetic energy storage system (SMES)

BESSs store electrical energy in the form of chemical energy between two or more chemical elements. They are DC power systems, hence the power electronics inverter is necessary for their connection to AC microgrids network. Currently, they are the most popular type of distributed storage and they still gain popularity.

Super-capacitors (sometimes ultra-capacitors) are storing directly electrical energy. Their biggest advantage is very high power density, the ability to tolerate frequent charging/discharging cycles and much shorter start-up times compared to batteries. Therefore, they can be used most efficiently in applications, where high power charging capability is more important than energy-storing [28].

Flywheel systems are converting electrical energy to rotation energy (kinetic energy). Usually, the system consists of rotation mass, electric motor supplying energy to it and generator coupled to the same shaft. Besides energy storage, this system can be also used for smoothing of different power sources.

The last type of energy storage is SMES. This system usually includes a superconducting coil located in artificially created extremely cold surroundings. Once the coil is charged the energy is stored in the form of magnetic energy nearly eternally. The charging and discharging losses are very low, thus the overall efficiency is mostly affected by the energy needed for creating the cold ambient [29].

2.1.2 Microgrids types

Depending on several parameters such as size, purpose, technical design, and stability aspects, the microgrids can generally be divided into few categories. [30, 31]

Utility microgrid

The utility or community microgrids (sometimes milligrids) are usually quite large microgrids that are connected to the main grid with the multiple PCC. The main microgrid network runs on medium voltage level so the PCC is provided by a high voltage (HV)/medium voltage (MV) power substation (primary substation). Community microgrids typically connect a few thousands of customers and bigger distributed generators such as wind power plants.

These microgrids do not deviate from the formal definition. Utility microgrid usually contains centrally owned distributed generators and the power balancing and control is realized by a central control system [32].

Remote microgrid

The remote microgrid is ordinarily not connected to the main grid and their geographical remoteness makes the connection to a macrogrid very costly or totally impossible. Hence, the microgrid system is usually controlled by decentralized control methods and stays in the islanded mode.

These microgrids can represent whole villages, small cities or grids on islands.

Facility microgrid

Facility microgrids represent the classical microgrid structure on a small scale. Mostly, it contains just one customer, private or industrial with small distributed power sources, for example, rooftop PV panels on private premises.

This type is generally connected with the main utility grid and works in grid-connected mode. Mostly just in case of faults in macrogrid, the mode would switch to islanded.

Institutional microgrid

Institutional, campus or virtual microgrids combines a group of low voltage distributed loads and/or distributed generators in such a way, that they can be observed as a single entity from the main grid point of view. From a system controllers point of view, this is a significant advantage.

Special cases

Besides these four cases, the microgrid concept can also be deployed in very special cases where the reliable energy supply is secured. A typical example of this problem can be the electricity network in military bases, hospitals or similar tactical objects.

2.1.3 Demand side management

In electricity systems where one significant part of the energy is created by renewable sources the new challenges arise. For stability purposes, the same amount of generated and consumed energy must be secured in the network for any moment in time. Usually, the peak of renewable generators does not correspond to the time of load peaks. For that reason, enough capacity of expensive back-up generators or other power sources must be located in the network.

One of the solutions to fit generation and load curve to each other a little better can be demand side management (DSM). Systems that apply DSM can reschedule the energy demand towards times when it can be covered more effectively.

DSM can be classified into two categories, direct and indirect load control. While direct load control increases or reduces the electric demand of assets, when the grid is imbalanced, indirect load control employs price signals and motivates the end customer to use electricity in specific hours by its price [33].

There are six load-shaping methods [34]:

1. Peak clipping - decreasing the maximum load peak value

2. Valley filling - filling the difference between peak and valley

3. Load shifting - moving peak load to the different place in time

4. Strategic conservation - reduction of general consumption because of future reasons

5. Strategic load growth - promotion of general consumption because of future reasons

6. Flexible load shape - increasing of load flexibility

In Figure 2.3 the load-shaping methods are visualized. It shows all six mentioned methods on the smaller figures. The purple arrows on all of them indicate the wanted change of the load curve.
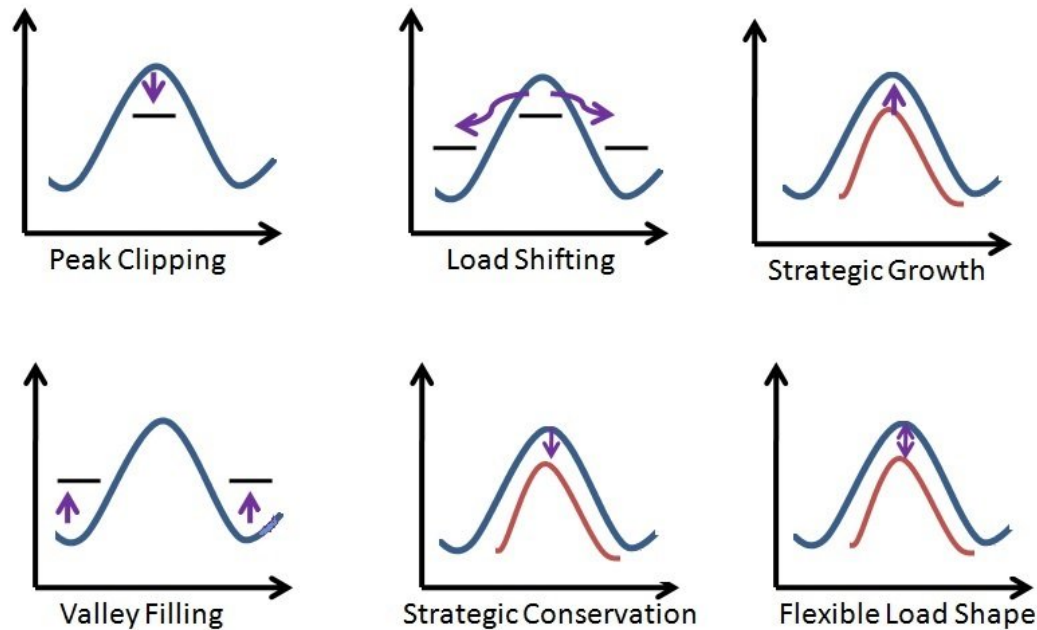

Figure 2.3: Illustration of load shaping methods [35]

Controllable loads

According to research in [36], one can classify controllable loads into three categories. Type I contains all smaller types of loads which are not critical for the end customers and can be interrupted or rescheduled. With this controllable load type, only the demand modification are possible, there is no energy to be stored and used later. Therefore, they are sometimes known as passive controllable loads. Typically, air-condition (A/C), water and central heating or washing machine processes can be re-planned to a later point in time.

There are two ways how to process this load management. The customer can make a deal with power utilities and then limit his power demand in preallocated time or when it is needed. The other approach gives the end customer a higher level of freedom. Short time-variant power prices are distributed between customers and they can adjust their power demand accordingly.

The second category, type II, is called active controllable loads and includes BESSs, vehicle-to-grid (V2G) systems, and combined cooling, heating and power systems (CCHPs). Unlike the previous category, these systems can store the generated energy for later use and supply it to the network.

The advantages of BESSs are described in Section 2.1.1. The development of V2G systems is strongly related to the rapid expansion of electro-mobility. In this concept, batteries of fully electric cars or of plug-in hybrid which are currently connected to the grid might be used as distributed storages when needed. These small capacity devices can help with power network balancing and provide support for distributed renewable generators. V2G can also be used as a controllable load of the first type by scheduling car charging.
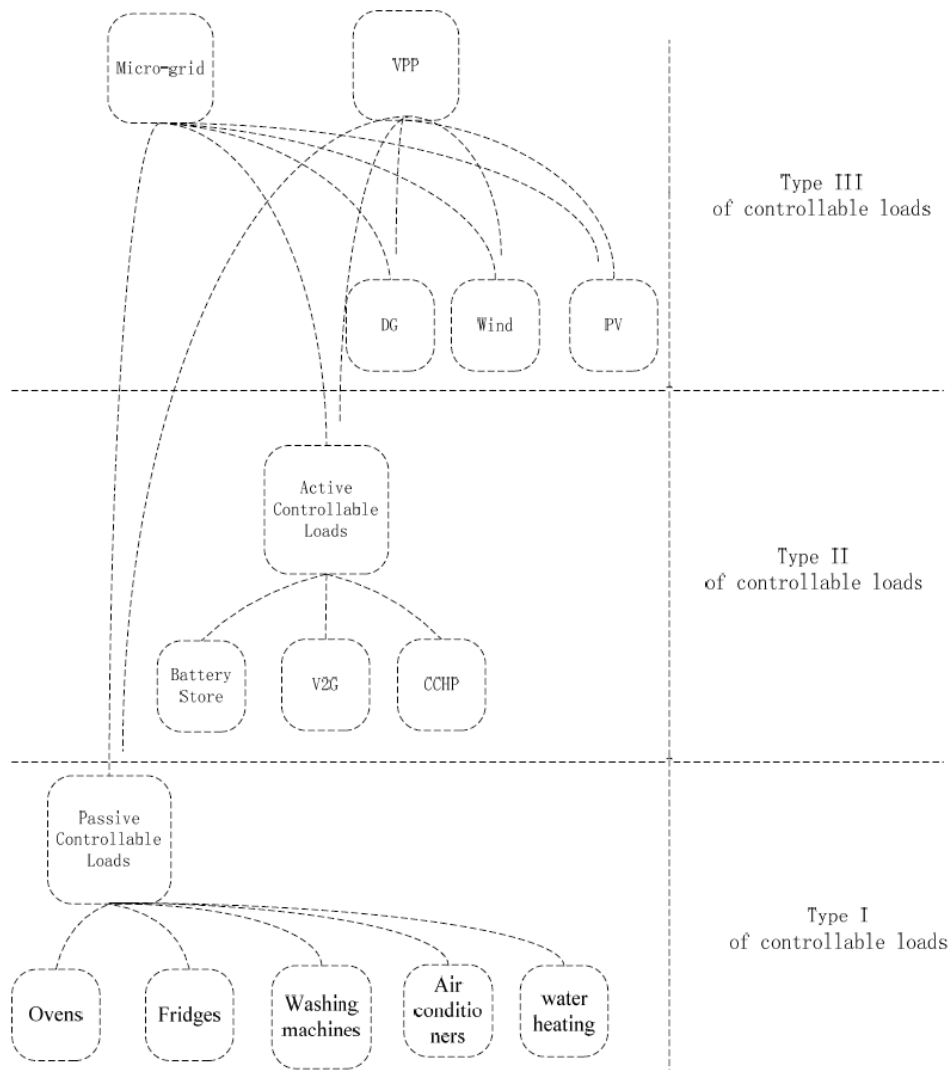

Figure 2.4: Classification of controllable loads [36]

CCHP saves energy into different end user's thermal processes such as space heating or cooling, water heating, refrigeration or in the case of industrial customers in the form of residual process heat. Due to the low criticality of these processes, the CCHPs are one of the most promising controllable loads.

In the last category, the whole microgrid or virtual power plant (VPP) (virtual object aggregating multiple DER and ESSs) is considered as a controllable load for the larger system. Besides the preceding load types, these systems also contain distributed generators. Described classification can be seen in Figure 2.4.

2.2 Typical microgrid controllers

Changing the power network infrastructure from the conventional grid structure towards the microgrid concept brings new challenges in its controlling systems. During grid-connected mode, the control might be done by the macrogrid operator and the microgrid central controller might only support this process and attempt to increase efficiency of the entire power generation process.

On the other hand, in the case of islanded mode, the microgrid's EMS must be able to provide voltage stability and general power flow quality regardless of intermittent power generation of renewable distributed sources.

Conventionally, the three-level-hierarchical control is used in case of power systems (including microgrids). The lowest level, primary control is in most cases designed as decentralized droop control which reacts to rapid load changes by changing the power output of AC generators.

However, these systems can reveal problems. The change of power output of a generator creates a trade-off between power change and general power qualities such as frequency or voltage. Moreover, this system is not obtainable for DC distributed generators which are irreplaceable components of microgrids. The primary control response is a very quick and autonomous operation. The time scale of this control is in the range of tens to hundreds of milliseconds to keep voltage and frequency close to nominal values.

On the contrary, the secondary control is mostly implemented in centralized or distributed form. This control operates in longer time-scale (seconds up to tens of seconds) and its main aim is to compensate the voltage and/or frequency offset introduced by the primary control.

The purpose of the highest control level, the tertiary control, is not to balance power generation and demand. Instead of it, it optimizes the performance of the grid according to economic and operational features. This is also known as the optimal power flow problem (OPF). Tertiary control can also manage all kinds of power flows inside of control area or in between more of them.

Usually, this level of control updates the control information quite seldom, approximately once every 15 minutes. In some implementation, this control structure is reduced to the two-layer and the features of the tertiary control are taken over by secondary control [5, 4].

This conventional control strategy does not take into account the distributed energy storages which are typical for microgrids. Similarly, the distributed power sources without mechanical rotating mass of large inertia are not possible to be controlled in the manner described above.

Therefore, the control strategies, especially for microgrids with energy storages and DC power generators, will be now introduced. In general, they can be classified into three groups based on their architecture. This classification can be noticed in Figure 2.5.

In decentralised control algorithms, there is no communication between components of the system at all. Each containing a local controller (LC) which is providing the decision making with only a local set of information. Due to the lack of this bonding between grid elements, the reaction time of the control can be very fast. Typically, the decentralized control is managed by the standard droop control or by droop control related to state of charge (SoC) of distributed ESS.

The centralised type of grid control adds a central controller to the system. The main goal of this central management is to adjust control levels of every single local controller and to provide the desired power set-points. Centralised control can be implemented in the secondary or tertiary control level.

Nevertheless, the centralized control brings up multiple challenges. In large systems where some microgrid parts are located in very remote areas, the communication distance might be enormous which is increasing controller reaction time significantly. The fact that all the information is stored at one location also introduces the problem of privacy, security, and reliability of the system. In case of a security breach to the central controller or in case of some kind of failure, the complete system might be shut down.

Hence, the third type of control is proposed. Distributed multi-agent system (MAS) control offers higher confidentiality for each microgrid component such as communication between direct neighbours in the network which makes the system faster and more reliable. The system might be also equipped with a plug-and-play feature that makes the connection of new agents to the grid very easy. In addition to that, the individual failure of one agent would lead to lower performance of the control, but not to complete collapse.

Similar to centralized control, distributed MAS can be used in secondary and tertiary control level. Recently, this type of control was in focus of many research studies and numerous different algorithms of distributed control were created. This topic is further discussed in Section 2.2.3 which is dedicated to it.

2.2.1 Decentralised control architecture

Since decentralized control can operate very fast it is usually used for the primary control, for balancing the frequency in the grid. As it was mentioned before, although the conventional droop control can be directly used in most of the microgrids cases, it can be slightly adjusted to provide efficient control for microgrid's distributed DC energy sources.
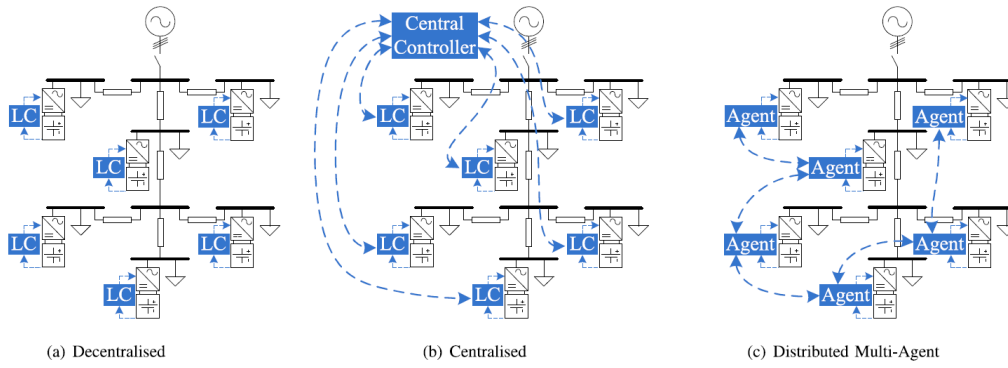
Figure 2.5: Decentralised, centralised and distributed multi-agent control architecture for microgrids (left to right) [5]

Three different adaptations of droop control are introduced in [5]. Besides classical version frequently used in macrogrid, there is droop control based on SoC of distributed ESS and one form of droop control for microgrids with heterogeneous storages.

Droop control

Conventional droop control is based on coupling between voltage frequency and amplitude and active and reactive output power. Since the power lines in microgrids are usually quite short and their impedance is mainly reactive, some elements of droop equations can be neglected and the control relationship is then interpreted by following equations (2.1) [9]

$$
\begin{aligned}
f_{MG} &= f^* - m \cdot (P - P^*), \\
U_{MG} &= U^* - n \cdot (Q - Q^*),
\end{aligned}
\tag{2.1}
$$

where U_{MG} and f_{MG} are frequency and amplitude of the microgrid voltage, P and Q are active and reactive power respectively and the variables with stars are base values. Constants m and n are droop coefficients. All the variables are used in per unit notation.

As it is seen from the equations 2.1, the output voltage frequency directly depends only on active power as well as voltage amplitude on reactive power. This approximation which can be done only in small scale systems makes the droop control very easy to implement.

For the connection of DC distributed generators to the AC grid the power inverters are needed. Typically, two types are used. voltage-controlled voltage source inverters (VCVSI) can to maintain voltage frequency and amplitude control. On the other hand, current-controlled voltage source inverters (CCVSI) provide active and reactive power control.

Both are ideal for different tasks. VCVSI can be used when the optimal power quality in terms of voltage amplitude and frequency is important. In contrast, CCVSI can be used in cases when power balance is not provided to return the system into a steady state [37].

SoC Droop control

Conventional droop control does not take the state of charge of distributed energy storages into consideration. The specific level of SoC which influences not only remaining energy capacity but also affects energy storage system efficiency and lifetime. For some systems, such as BESS, it might be very inconvenient to discharge stored energy completely due to the faster ageing of batteries [38].

One of the described solutions of this problem implements weighted droop coefficients into the droop equations. As a result of this, the energy storage system with higher SoC can be prioritized and the probability of very low SoC of any of the ESS is lowered. Therefore, the power demand could be split between ESSs more advantageously.

This system still has some constraints. In case when one ESS has significantly higher SoC then another, it would be preferred and rapidly discharged with high discharging current to cover the power demand. However, the discharging current is limited in most of the ESS applications. Secondly, it is quite obvious that in case of low SoC of all ESSs that voltage amplitude and frequency control would be affected.

Heterogeneous storage droop control

Currently, there is no single energy storage type that would be able to secure effective and low-cost energy for all the processes in the microgrid. Hence, the microgrid architecture usually contains multiple various types. This brings diversity into the grid and enables efficient govern to the control algorithm. These systems are often referred to in literature as hybrid energy storage systems [39].

To utilize different energy storages described in Section 2.1.1, it is useful to consider their specific properties. Various ESSs can differ in many parameters such as specific power density, energy density, energy price or cycle life. Each ESS composition is designed for different operation purposes.

For example, supercapacitors are the type of energy storage with long cycle life, high specific power density, but quite high energy price as well. Therefore, it can be used very efficiently for power balancing in the grid, however, they are completely inappropriate for delivering constant energy for a longer period.

There are numerous control algorithms for this type of microgrid system. Among the most interesting: embedding the linear filtering into the grid. In this algorithm, the power demand signal is filtered with a low pass filter and then divided into short-term fluctuation and long-term power demand signal accordingly. Subsequently, the fast-cycling ESSs such as supercapacitors cover the low grid power variation and i.e. BESS secure the stable power output.

2.2.2 Centralised control architecture

The second type of control strategy is built-in centralised way. Centralised controllers are usually implemented as a secondary or tertiary control providing power quality control and optimal power flow supervision.

In general, these algorithms can be divided into these two hierarchical control categories, secondary and tertiary.

Secondary control

Conventionally, the centralised controller as a secondary control is used for correction of deviation from desired voltage amplitude and frequency created by setting the correct power set-points. There are several algorithms presented in [5] modified especially for microgrid usage.

Certainly, the classic secondary control as it is known from the use in macrogrid can be adapted to microgrids with distributed energy storages by taking BESSs of individual storages into consideration by providing weighted droop control as it was described in Section 2.2.1. However, it does not solve the problem of overloading of the most charged storage in case of low SoC on others.

Another useful approach is balancing discharge rates of joined energy storages. Always when there is generated power shortage, the missing power is split into ESSs inequitable way such that all storages can discharge at the same speed. This algorithm works reasonably fine if the initial SoC of the storages is the same. However, it does not take into consideration different properties of ESSs and their advantages and disadvantages.

The lifespan of battery packs in BESS depends, among other parameters, on charge/discharge cycles and depth of each discharge process. To improve this factor a new method is designed that starts a charging process for each ESS component when the batteries reach a float voltage. Thus the number of charging/discharging cycles is minimized and the lifetime of the battery packs is extended.

The last presented algorithm is the rule-based control. With this set of rules, the microgrid is maintained and optimized as much as possible. It might include the decision making for many possible states of the system including fault states. Previously described algorithms can be also combined by rule-based algorithm to use them in their most advantageous time.

Tertiary control

Tertiary control in the microgrid concept has different goals during grid-connection mode and islanded mode. What remains unchanged, is the optimization of power flow between individual components and the effectiveness of the whole grid.

During grid-connection, the optimal power flow between the microgrid and main macrogrid could be optimized in such a way, that it is most economically beneficial. The energy price in the macrogrid can be taken as it is from a local utility or it can be predicted by an algorithm such as model predictive control. Under consideration

of this information, the power flow through the PCC can be optimized by buying energy and charging distributed energy storages during cheap electricity periods. Similarly, power can be supplied to the main grid when there is a surplus in the microgrid or when it is economically preferable.

In contrast, during islanded mode, the general aim of tertiary control is different due to no power exchange with the main grid. In this case, the controller can focus on forecasts of power generation of renewable sources and an optimal dispatch. For example, in some periods of the day much larger contribution of PV power resources can be expected. Similarly, the load curve can be estimated and charging or discharging of ESSs can be planned accordingly.

2.2.3 Distributed multi-agent control architecture

The last group of control system architectures includes algorithms which appear to be very promising for further research. In comparison with the previously described hierarchical control architecture, the distributed MAS control offers many advantages [9, 5, 8].

That is the reason why they are commonly used not only in power grid systems but also in computer science, sensor networks or for groups of unmanned vehicles such as flying drones or other types of ground robots [40].

As the name implies, this approach is based on splitting the microgrid into smaller pieces, usually to model each component as an independent agent which unfold many typical features. Firstly, the complexity of the control is quite low. Each agent can work separately with an own set of information and security that this approach provides. The fact that it does not depend on anyone else also increases the reliability significantly.

However, in comparison with decentralized control methods, the communication and data exchange between individual agents is possible. Therefore, each agent simply behaves according to its information about surroundings, responds directly to the changes and can fully employ the distributed resources and storages.

This communication network is ordinarily sparse, such that there is no connection between each agent but only in between selected ones (for example neighbouring agents). Thanks to that, the agents face a reduced amount of communication effort. Furthermore, communication is usually done on short distances and therefore can be very fast [5]. There are three different communication architectures which will be discussed later in Section 2.2.3.

In addition to it, the system is highly adaptive to the changes in communication or power connection topology. In case that the topology is still connected after the adjustments, the system should be able to adapt.

Similar to a centralized algorithm, distributed MAS can be deployed for secondary and tertiary control. As secondary control, the agents are sharing their information with their neighbourhood and organize the load sharing.

In the case of tertiary control, many algorithms with cooperative or competitive approaches to agent behaviour can be found in literature. Algorithms from both of these categories will be further discussed in Section 2.2.3.

Communication architecture

The communication between individual agents in the networks can be provided according to three different architectures, hierarchical, topology-based and fully distributed. Exemplary diagrams for each of the architecture are given in Figure 2.6 [5].
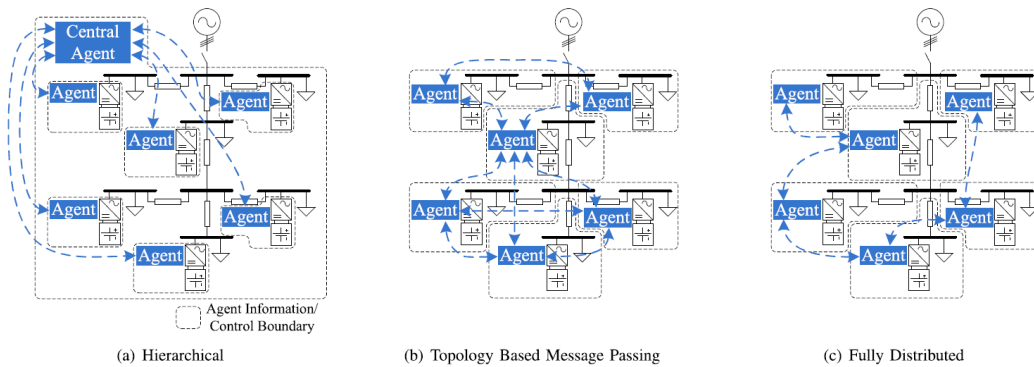

(a) Hierarchical   (b) Topology Based Message Passing   (c) Fully Distributed

Figure 2.6: Distributed MAS communication architectures [5]

First of all, in the hierarchical architecture, all the agents communicate with each other through one central agent. It can be a randomly chosen one from the agent set or a new agent added to the grid exactly for this purpose. The central agent is aware of the grid topology and allocating the optimization problems to each agent.

Even in the presence of the central agent, each agent works with its own set of parameters, objective function and constraints. The information distribution is the main difference between this algorithm and centralized control algorithms, that were introduced in the previous section.

The second architecture enables agents to exchange data directly only with neighbours based on the network topology. Usually, this communication network precisely mirrors the power network connection. Therefore, it is normally the most cost-efficient way to establish a communication connection.

Each agent is aware of its neighbours and the parameters of the power connection. Hence, the complex problem of optimal power flow can be distributed between them. The agents are usually iteratively updating their local variables and converging to a consensus. This algorithm is further discussed in the following chapter.

The last communication architecture is fully distributed and it contains communication connection between all agents. It is *de facto* a specific modification of the topology based architecture.

This architecture is advantageous for its high robustness, not only due to the potential failure of one of the agent but also for total independence from the power network topology. However, it is usually the most complex and expensive to construct.

Control strategies

There are several strategies of MAS control based on many different approaches. Demonstration of synchronization of independent agents could be found often in nature. Based on observation of schools of fish or flocks of birds, many of these algorithms were created [7].

First, the big class of these strategies is containing consensus algorithms which are providing synchronization of the agents. These algorithms are iteratively looking for a common value of defined parameters by the cooperation of the agents.

The other group of control strategies contains algorithms based on game theory. Game theory algorithms are creating an environment in which all agents are considered as players of the game and they are trying to optimize their objective depending on their and other players' actions simultaneously. If the goal of each agent can be expressed, game theory control algorithms can provide a large set of interesting solutions [8].

Solely the consensus algorithm will is described in detail in the following section.

Consensus algorithms

Consensus algorithms are control strategies that are described as interaction between neighbouring agents in one network topology to convert to the optimal value of specific shared variable. In case that the agent can be described as single integrator systems, the dynamic of consensus algorithms in discrete system can be expressed by equation (2.3) [16]

$$x_i[t+1] = \sum_{j=1}^{n} d_{ij}x_j[t], \tag{2.2}$$

where x_i and x_j both describe local information of agent i and j respectively, where agent i is the examined agent and agent j is part of a set of neighbours n. The constant d_{ij} stands for a coupling coefficient between these specific agents and t indicates time step.

In case that the network connection graph is in the form of a spanning tree and it is fully connected, the consensus is achieved. Although, the system dynamic highly depends on d_{ij} coefficients. Therefore, correct settings of them is crucial [41].

Equation (2.3) can be described in matrix form to state one time-step computation of the whole network into one

$$X[t+1] = DX[t], \tag{2.3}$$

where D matrix is a weighted adjacency matrix (communication matrix) of the system, it is symmetrical over the main diagonal and contains d_{ij} communication coefficients between individual agents.

It can be designed in different ways which highly influence the final performance. For some topologies, such as radial or ring connection of agents, it might change the dynamics significantly [42]. The selected variants are further discussed in Chapter 4.

Since consensus algorithms can be described as an integral part of the MAS networks, there are many different adaptations to the specific needs of each network. To modify the algorithm for real networks, consensus strategy with delays as well as with changing topology and with sampled data are discussed.

Beside that, the optimal consensus, adaptive consensus algorithm is presented in [9] to achieve better control performance. Depending on which type of system the agents are located in, the consensus for single-integrator systems and second-order consensus algorithm can be found. Besides, algorithms for generic linear system agents are mentioned.

Moreover, the consensus algorithm can be modified by adding a leader to the system to improve the control performance. Leaderless systems convert to a consensus based only on their initial values. Declaring one agent as a leader changes the dynamics a bit and the common value is then pinning to it.

This changes the problem from a cooperative regulator problem to a cooperative tracking. On the other hand, pinning consensus algorithm is not applicable when the right final value is unknown [7].

2.3 The Concept of model predictive control

MPC is a control strategy firstly used in the 80s in the petrochemical industry. After that, it was thoroughly investigated and massively deployed in many other industrial fields [43].

In literature, MPC is also known as dynamic matrix control, generalised predictive control, model algorithmic control or predictive functional control. Therefore, the model predictive control is the generic name which covers all these control systems together.

There are many reasons for MPC popularity. MPC control can provide multivariable control solutions and take the physical limitation of the system into consideration. Besides that, it allows the system to operate, considering physical limits or very close to them which makes it usually very effective.

Lastly, the update rate of individual steps is not that fast and therefore there is sufficient time for computation that has to be done during the control. This reason was crucial mostly at the start of the first MPC implementation due to the lower computation power than we have today. In these days, this is only a minor advantage of the algorithm [10].

Control structure is generally quite simple. Essentially, the controller has to contain a dynamic model of a controlled system which is used to forecast the future states. This allows to MPC to take into consideration the future evolution of state variables during their optimization in the current time. Thanks to that, MPC can predict future events and optimally prepare for them unlike classical proportional–integral–derivative control (PID) control.

For the performance of the algorithm, it does not matter how was the model obtained. Generally, it is more convenient to use linear time-invariant (LTI) models if possible. When the system does not have linear dynamic or if it can not be linearised reasonably, the version of non-linear MPC is also available. However, in the case of LTI model, the control problem is simplified with linear algebra principles and the complexity of the problem is reduced to the matrix equations, which can be computed very fast and efficiently [44].

Often, the model is just an approximation of the system and has smaller or larger differences in its dynamics. Hence, there is always some level of uncertainty in the prediction. To decide how should the algorithm proceed, a cost function is introduced. This function solves the typical trade-off between the performance of the system and the price of the control. That can be described as the ability to follow the right trajectory and price of the input to the system, respectively. This function is usually designed according to what is important for the system and control designer.

When the future strategy is completely planned, only the first step of the control is applied. Subsequently, the whole control process is repeated in the next time step and the prediction horizon is also moved one step forward.

In real life systems, the resources are always limited. Luckily, the algorithm is aware of constraints in the size of the input to the system as well as in state values. These constraints can be classified into two categories, equality and inequality constraints.

As an illustration, the first group contains any relationship between state variables that must be precisely held at any time. The second category represents for instance maximum possible input to the system which can not be exceeded.

In Figure 2.7 some significant signals of MPC control in the current time step k are shown. Signal $s(t)$ represents the set-point of the system, the value to which the actual output $y(t)$ should converge. Signal $r(t)$ stands for reference trajectory in the time step k. It shows the optimal trajectory that the system should follow.

The internal model of the system is used to create predicted outputs $\hat{y}(t|k)$ and $\hat{y}_f(t|k)$ with applied input and without it respectively. As it is visible, they depend on current time-step k. Afterwards, the $\hat{y}(t|k)$ can be expressed as a free system response $\hat{y}_f(t|k)$ and the response depending on the applied input. From this relationship, the optimal applied input can be easily computed.

As was said before, from the computed optimal input just the first step is taken and the whole process is repeated for the next time-step. For the sake of simplicity, the presented example is a single input single output continuous system. In the case

of the multi-variable control system, the reference signal $r(t)$ is often computed as least square permeation of single references.

For the case of MPC with constraints, the more complicated algorithms for reference computation can be used. The predicted outputs are computed for multiple time steps and then the least square algorithm concerning the constraints is applied. In the end, just the first step of the computed trajectory is taken, as always [10].

For this thesis, the description of the MPC algorithm in case of linear time-invariant systems will follow.

2.3.1 MPC formulation

In general, the MPC algorithm proceeds in three steps; it measures the available measurements, computes the optimal input accordingly and then applies it to the system. The controller performance can be influenced by two important components of MPC structure.

Firstly, the definition of an internal model and the fact how it reflects the reality significantly determines the speed with which the controlled output can converge to the reference. Secondly, the definition of the cost function solves the trade-off between different aspects of the controller. The designer of the control can typically decide what is the priority, the cost-saving of the input to the system or the speed of controller convergence.

The typical implementation of MPC control can be seen in Figure 2.8. In this case, it is enhanced by the observer which is a classical implementation of a Kalman filter. These settings can be used when the system is not fully observable.

Internal model

For this thesis, the linear time-invariant discrete-time model will be assumed.

In the general implementation of the MPC algorithm into the real world, the systems are usually non-linear and continuous where there are no assumptions applied. In it is the case, the system must be a priori linearized on some reasonable surroundings (usually around equilibrium points). Moreover, it has to be sampled.

Applying state-space equations the model can be described by equations (2.4) [10]

$$\begin{aligned}
x(k+1) &= Ax(k) + Bu(k), \\
y(k) &= C_y x(k), \\
z(k) &= C_z x(k),
\end{aligned} \qquad (2.4)$$

where x is a vector of the state variables, y is a vector of measured outputs and z is a vector of controllable outputs. In ordinary system type, the vectors y and z are the same.

For LTI system, it does not matter how the internal model is obtained. One of the possible ways is the identification regarding system response. Other possibilities are trying to approximate the real system with known system equations or to declare it as a known system and then identify its parameters.

Cost function

The cost function assigns scalar prices to each possible control strategies. The optimal one is then chosen as the control strategy with the lowest cost. Usually, quadratic cost functions are used due to their simplicity and ensured non-negative values. In general form, the cost function can be defined as equation (2.5) [10]

$$V(k) = \sum_{i=H_w}^{H_p} ||\hat{z}(k+i|k) - r(k+i|k)||^2_{Q(i)} + \sum_{i=0}^{H_u-1} ||\Delta\hat{u}(k+i|k)||^2_{R(i)}. \qquad (2.5)$$

This equation contains two terms. The first one penalizes the distance between predicted output of the system $\hat{z}$ and reference r for each future time step in dependency on current time step k. That is done by summation of all penalties in prediction horizon H_p. The first penalized time step is set by H_w.

The second term penalizes the used input into the system for each time step in the defined control horizon H_u, where $H_u \leq H_p$. Both equation terms are multiplied by coefficients Q and R, respectively. With these factors, the weight of each term can be defined. In the case of single controlled variable systems, these two parameters are scalars, but in the case of general multi-variable systems, they are matrices. They both are assumed to be non-negative and even more often diagonal.

Constraints

The inequality constraints of the system are defined in matrices E, F, and G and taking restriction of input change $\Delta\hat{u}$, input absolute value $\hat{u}$ and controlled variables $\hat{z}$ respectively into consideration.

The matrices have the structure so the following matrix equation would create each constraint in each line of the final equation,

$$E \cdot \begin{vmatrix} \Delta\hat{u}(k|k) \\ \vdots \\ \Delta\hat{u}(k+H_u-1|k) \\ 1 \end{vmatrix} \leq \begin{vmatrix} 0 \\ \vdots \\ 0 \\ 0 \end{vmatrix}. \qquad (2.6)$$

The structure of the other two matrices is based on the same principle.

2.3.2 MPC solution

In this section, the differences between constrained and unconstrained solutions of the controlled system are discussed. Although there are differences between these two approaches, they are both based on minimization of the cost function.

Unconstrained solution

As said before, in the unconstrained case the solution of the minimization can be reduced to the matrix operation. The cost function can be modified as follows [10]

$$V(k) = ||Z(k) - T(k)||^2_Q + ||\Delta U(k)||^2_R, \qquad (2.7)$$

where Z, T, and ΔU are column vectors of $\hat{z}$, $\hat{r}$, and $\Delta \hat{u}$ in each time step of the predicted horizon.

Furthermore, Z can be written in the form that reveals the dependency on current state, input, and change of the input from the last time step,

$$Z(k) = \Psi x(k) + \Phi u(k-1) + \Theta \Delta U(k). \tag{2.8}$$

Subsequently, tracking error ϵ can be defined as the difference between predicted free response of the system $\hat{y}_f$ and predicted trajectory $\hat{r}$. This error shows the progress of control if it is equal to zero the control reference is reached,

$$\epsilon(k) = T(k) - \Psi x(k) - \Phi u(k-1). \tag{2.9}$$

From here the cost function can be redesigned as follows

$$V(k) = const - \Delta U(k)^T G + \Delta U(k)^T H \Delta U(k), \tag{2.10}$$

where G and H are defined as

$$G = 2\Theta^T Q \epsilon, \tag{2.11}$$

$$H = \Theta^T Q \Theta + R. \tag{2.12}$$

The optimal input to the system $\Delta U(k)_{opt}$ is then found by minimization of equation (2.10). The gradient is computed and set to zero. The final form of the optimum input is then defined in equation (2.13)

$$\Delta U(k)_{opt} = \frac{1}{2} H^{-1} G. \tag{2.13}$$

There is another way, based on the least square algorithm with which it is possible to compute the optimal input. Since the inverse matrix of Hessian matrix H can be quite tricky, this approach is mostly used.

Firstly, the square roots of R and Q matrix are necessary,

$$\begin{aligned} S_Q^T S_Q &= Q, \\ S_R^T S_R &= R. \end{aligned} \tag{2.14}$$

Based on them, the square root of the cost function can be found,

$$\left| \begin{matrix} S_Q(\Theta \Delta U(k) - \epsilon(k)) \\ S_R \Delta U(k) \end{matrix} \right|^2 = V(k), \tag{2.15}$$

and the least square solution of this equation

$$\left| \begin{matrix} S_Q \Theta \\ S_R \end{matrix} \right| \Delta U(k) = \left| \begin{matrix} S_Q \epsilon(k) \\ 0 \end{matrix} \right|. \tag{2.16}$$

Constrained solution

All three constraint matrices can be expressed in the same fashion as matrix F

$$\begin{vmatrix} F_1 & F_2 & \dots & F_{H_u} & f \end{vmatrix} \cdot \begin{vmatrix} \hat{u}(k|k) \\ \vdots \\ \hat{u}(k + H_u - 1|k) \\ 1 \end{vmatrix} \leq \begin{vmatrix} 0 \\ \vdots \\ 0 \\ 0 \end{vmatrix}. \tag{2.17}$$

Since the predicted input can changes to form of equation (2.18) the matrix F can be rewritten as equation (2.19),

$$\hat{u}(k + i - 1|k) = u(k - 1) + \sum_{j=0}^{i-1} \Delta\hat{u}(k + j|k), \tag{2.18}$$

$$F\Delta U(k) \leq -F_1 u(k - 1) - f. \tag{2.19}$$

Now, the same trick can be used for the constraint matrix G. For which the decomposition according to equation (2.8) is used. After setting $G = \begin{vmatrix} \Gamma & g \end{vmatrix}$ it can be finally expressed similarly in equation (2.19),

$$\Gamma\Theta\Delta U(k) \leq -\Gamma(\Psi x(k) + \Phi u(k - 1)) - g. \tag{2.20}$$

All constraints can be summed up in one equation (2.21),

$$\begin{vmatrix} F \\ \Gamma\Theta \\ W \end{vmatrix} \Delta U(k) \leq \begin{vmatrix} -F_1 u(k - 1) - f \\ -\Gamma(\Psi x(k) + \Phi u(k - 1)) - g \\ w \end{vmatrix}. \tag{2.21}$$

Above-mentioned, the optimum input is found as a minimization of cost function, in this time as a subject to constraints in equation (2.21). This kind of optimization problem is called quadratic programming (QP) and it is a standard optimization algorithm. Here, the task is presented as the following minimization,

$$minimize\ \Delta U(k)^T H \Delta U(k) - G^T \Delta U(k). \tag{2.22}$$

The solution of the QP problem is shown in [10]. Due to the high complexity, it is not further discussed in this work.
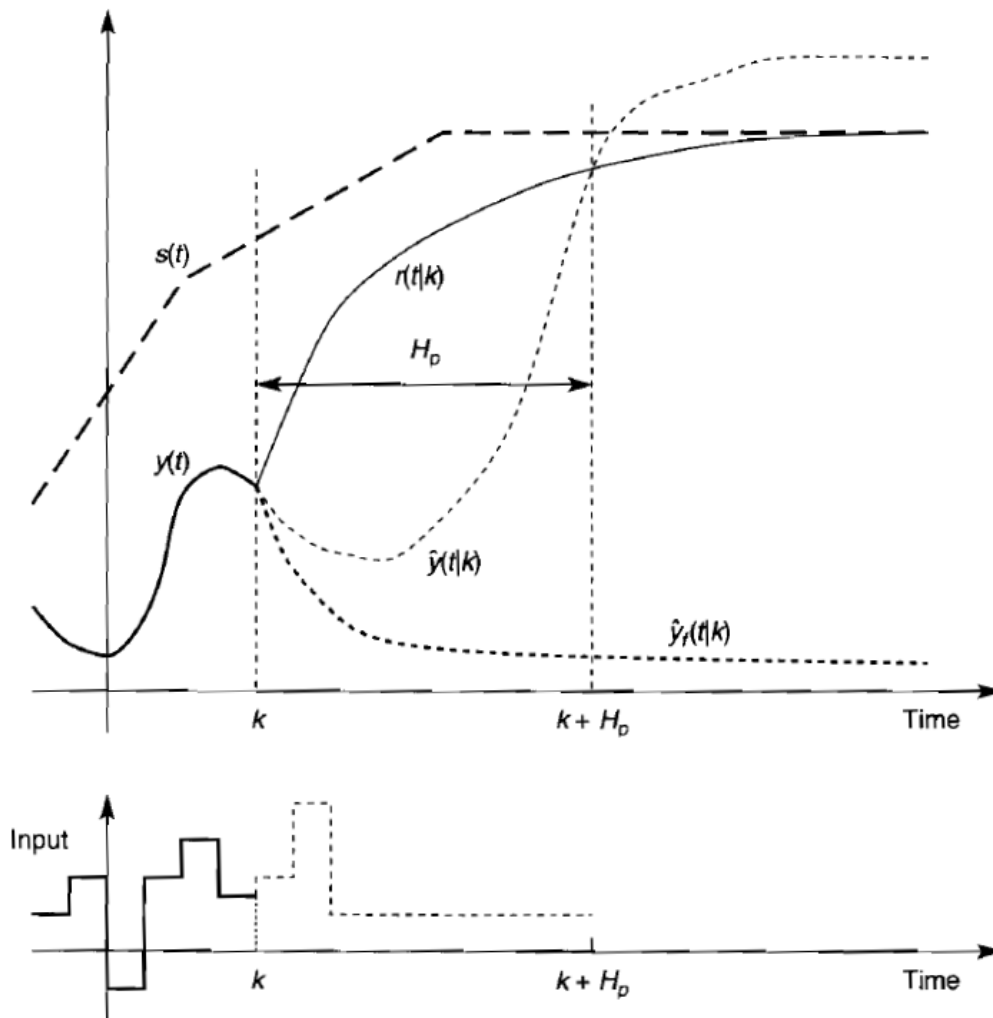
Figure 2.7: Basic idea of MPC shown on dependency of individual signals on time
[10]
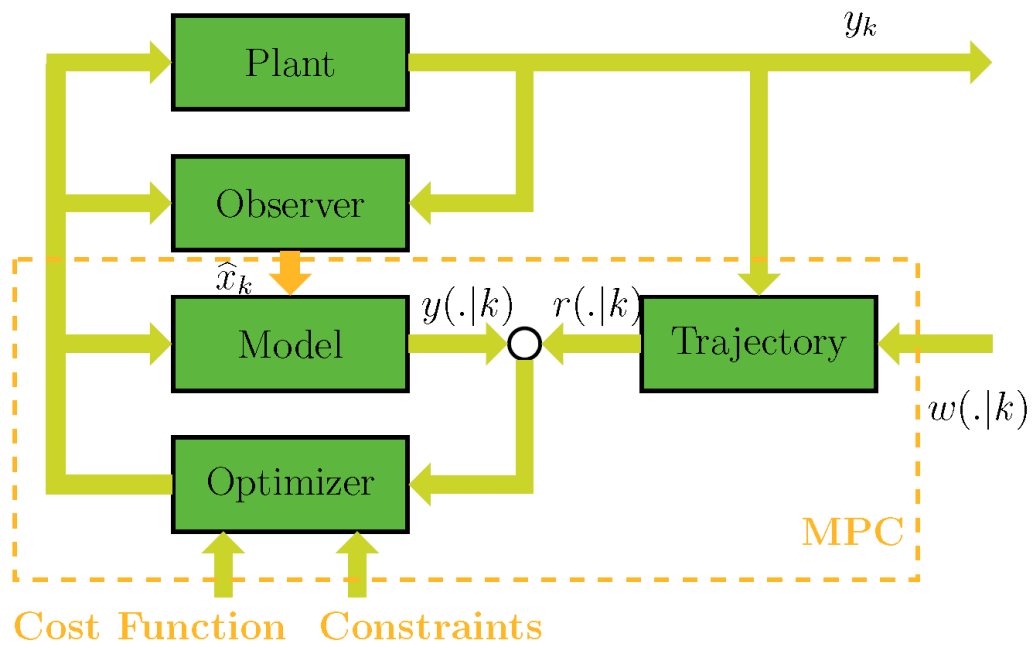
Figure 2.8: Structure of MPC enhanced by observer (when some of the states are not observable from system outputs). In this case the set-point of the system is labelled as $w(.|k)$ [45]

3 Use Case

For the rigorous validation of the created control algorithm, the testing on the data from the real-life demonstration site is necessary. Thanks to that, the real phenomena, which can occur in the microgrid, can be observed.

In the context of H2020 EU Projekt InterFlex, the consortium develops advanced control solutions for the microgrid test site in Simris, developed by E.ON in Sweden.

The testing of the software in the authentic environment brings the opportunity to test the control algorithms on the situations, that would occur very rarely in real-life, but could be critical for the whole system. That increases the final reliability of the analysis, proposed solution of the project and creates the ideas for the further development and reasoning for a future deployment of these new control schemes.

3.1 Demonstration site Simris

The test site *Simris* is located in southern Sweden. It is a microgrid concept, capable to run all by itself which contains distributed renewable sources, distributed storage systems and connections to the communities nearby this village. The project started in 2017 and since then, it was used for testing new features of microgrid and smart grid concepts and also for testing of large variety of control algorithms.

3.1.1 Simris components

The structure of *Simris* can be seen in Figure 3.1. The individual components of the microgrid are represented by their schematic symbols [15].

In the right bottom corner the renewable sources, PV park, and wind generator are illustrated. Right above them, the BUG and BESS can be seen. All of these components have assigned transformers for the conversion of their output voltage to the grid level. Of course, due to the DC output voltage of the PV park and BESS, there are additionally DC/AC inverters.

The installed rated powers of the PV park, wind generator and BUG are 500 kW, 442 kW, and 350 kW respectively. In the original implementation of the BESS, the battery pack was constructed with Li-Ion batteries with a total capacity of 333 kWh. In early 2019 the redox flow BESS was added parallel to the already implemented BESS. It increased a total battery capacity of the system up to 1933 kWh.

The figure also depicts six schematic symbols of accumulated loads, which are together representing 150 objects, mostly households. Couple of them are equipped by distributed energy storages which opens the opportunity for demand side manage-

ment. Currently, the water boilers, heat pumps, and distributed BESS are installed with a total capacity of 142.55 kWh.
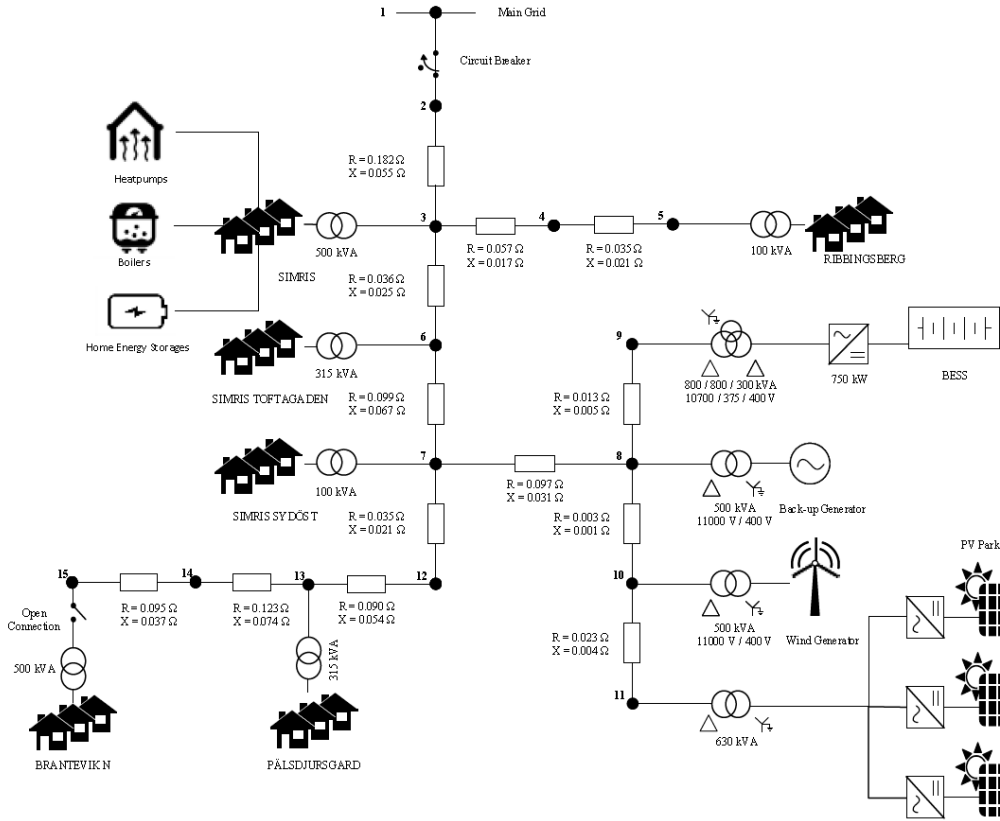
Figure 3.1: Schematic structure of *Simris* demonstration site [15]

On the top of the figure, the PCC with the macrogrid is shown. There are also additional components of the microgrid structure such as circuit breakers. In between individual components, there are black numbered dots that represent physically installed buses. The parameters of each power bus, such as resistance and reactance are also listed.

3.2 Measured data

For the simulation of the designed controller, not all measurements of the highlighted buses are needed. It is only necessary to collect the measurements of seven "passive" nodes, power measurement from buses 3, 5, 6, 7, 10, 11 and 13. The control concept and reasoning behind this decision will be further discussed in Chapter 4.

Unfortunately, the work with real-life data brings some problems. Firstly, not all the data can be used. For the successful simulation of the control, the measured data should be taken simultaneously. It is also useful when the individual measured

data vectors are sampled with the same sampling frequency. If this is not the case, the data has to be extrapolated or re-sampled to obtain the same measuring times.

Another usual problem is missing some data. In the real-life measuring systems the successful rate of measuring systems is nearly never 100%. The solution of this problem might be once again the extrapolation.

In this specific case, the necessary data from bus 10 are not available. Instead of it, there is a data vector measured on bus 8 which contains the sum of data from bus 10 and 11. Therefore, this does not have to be considered as a problem. To get the requested data from bus 10 we can simply subtract vector 11 from measured vector 8.

The data selection aimed to find a period that is as long as possible with as fast as possible sampling rate. From the given data, the period of 33 days between the afternoons of 3.9.2017 and 4.10.2017 is chosen. Five of the measured nodes were measured originally with sampling time 10 seconds, the other two were measured faster, every 1 second. Therefore, they are re-sampled to the same frequency.

For this time interval, all the measured vectors should have a length equal to 268 976 samples. The description of the measured data is shown in Table 3.1:

Bus number	Name	Data length	Missing data [%]
3	SRS 131	268 669	0.11
5	SRS 204	268 908	0.03
6	N 149 464	268 976	0
7	N 115 765	268 923	0.02
8	N 149 403	237 120	11.84
11	N 140 359	267 530	0.54
12	N 106 160	265 381	1.42

Table 3.1: Table showing the amount of missing data in measured vectors

As it is clear from the rates of the missing data, there is no problem in the extrapolation of the missing data for most of the measured vectors. Unfortunately, the vector measured at bus number 8 is missing a significant amount of data, approximately 3 days.

Since it represents the summation of the data from PV farm and wind generator, the vector is in the shape formed by PV farm data, it looks like a typical curve highly dependent on the time of the day.

That is why in the control simulation, 3 days of data before the data gap are multiplied once again behind it to fill the gap.

After this correction, the rest of the data is fixed applying the *MATLAB* function *fillmissing* [46] that provides piecewise cubic spline interpolation. With this correction, the continuity of the data is preserved and measured vectors are extended to the same length.

3.3 Other used data

Besides measured data on the test site, another data set is necessary for the control algorithm. For the right settings of the cost function parameters, the price of energy generated from individual sources during the measured period must be known.

Information about global energy prices are taken from the official database of *Nord pool* energy market past data that are freely accessible through their web-page [47]. For the area of Sweden where *Simris* is located the day-ahead settlement energy price is available every hour. Therefore, they have to be also extrapolated to the desired sampling frequency.

The past price of the BUG fuel in Sweden in autumn 2017 can be also found on-line [48]. The consumption of the BUG can be assumed to behave linearly concerning the created power [49], hence computation of the energy price created by this method is not complicated.

3.4 Reference control algorithm

For the comparison of the suggested control algorithm with a comparable control structure, another control strategy that is utilizing BESS is needed. This additional control approach is necessary to provide a reference rule-based control to manage the BESS in the microgrid system.

Therefore, one of the simplest control approaches is created. The general idea is to charge and discharge BESS between its limits with constant charging and discharging power. Thus, the power from BESS would be in the form of the square function over the time simulation, the BESS SoC would form the triangle function and the battery pack would be utilized during all time steps.

The implementation of this control is done by simple relating of BESS cost function parameters to the global energy price. In the beginning, the cost of BESS is set a little bit lower, given a fixed term. At the moment of reaching the BESS SoC limit, the value is multiplied by -1 and the utilization of power from the battery pack turns out to be more costly than from the main grid. When reaching the upper limit, the value changes again its sign and the whole process is repeated.

In consideration of the BESS energy capacity, the described value is experimentally chosen as 3 €/MWh. With these settings, one full equivalent battery cycle is done in time duration approximately one day.

The SoC of BESS in the third week of the measured period between 18.9.2017 and 25.9.2017 is shown in Figure 3.2. It can be seen that the displayed function does not completely follow the shape of the triangle function. This light differentiation is caused by the influence of renewable sources and their variable production.

Nevertheless, this effect does not restrict the usability of the reference control. Moreover, the later discharging in the case when the microgrid energy sources produce more power than needed is meaningful and simulates the real situation accordingly.
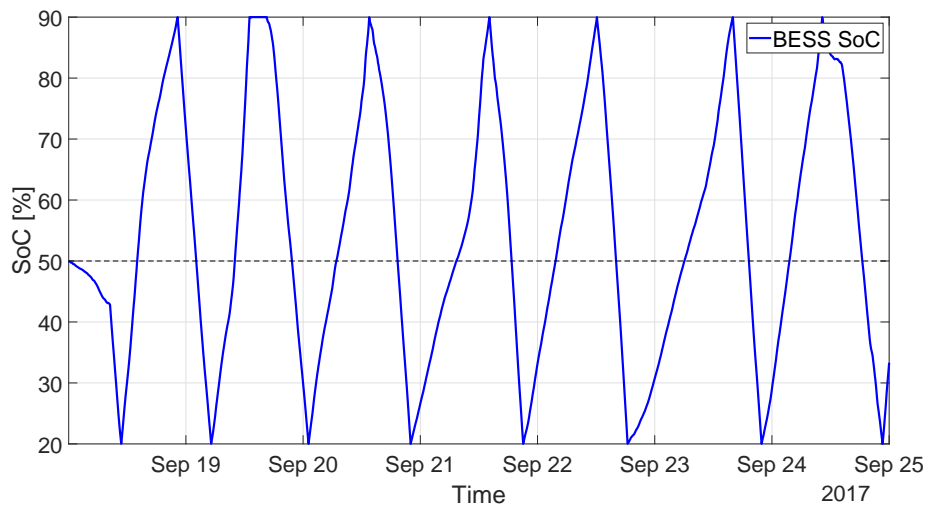
Figure 3.2: SoC of BESS during one week test with reference control

4 Modelling the Controller

As the main objective of the thesis, the control mechanism for the described system in Chapter 3 is designed. The fundamental ambition of the controller is to provide the economical optimality of the system during the power balancing of the grid.

The designed controller can be divided into two layers. In the bottom one, a distributed multi-agent system is used for the administration of the power distribution between individual power sources. This control works at considerably high speed and is executed every 10 seconds. Therefore, it represents a conventional secondary control level.

This type of control is chosen due to its high process reliability, computation speed and the ability of the system to react to eventual changes in the network topology. Thanks to that, the system is an ideal control mechanism for finding the appropriate power distribution ratio between power sources and it ensures the power balance.

However, this lower algorithm level aims only at providing optimal power distribution from the theoretically infinite distributed sources. However, this does not represent the real-life case and the sources are limited not only in rated power but in the case of BESS in the power capacity as well.

This problem may lead to the exceeding of the output current from the sources, which may prove to be very critical. Moreover, heavy discharging of the batteries may strongly affect the process of ageing which is not desirable.

For these reasons, the upper level of control is implemented. The model predictive controller considers all the constraints into consideration that the real-life systems brings and additionally, it optimizes the charging and discharging processes on the BESS.

Every 15 minutes, the future development of the battery pack state of charge is predicted and the optimal control input is chosen accordingly. Hence, the MPC controller represents the tertiary control in the traditional representation.

Employing this control configuration, the network operator can determine the emphasis on the SoC of BESS or the price of the power received from the main power grid. Also, under consideration of forecasts for the distributed renewable energy sources, the optimal charging and discharging in time of expensive power price can be realized.

This brings to the system the necessary economical optimization and it enables the grid operator to consume the locally generated green energy efficiently without unnecessary wasting. These aspects are crucial for the usability of the microgrid concept and its further deployment in the future.

4.1 Control structure

For the sake of MAS control, the physical system that is shown in Figure 3.1 has to be divided into individual agents. This classification can be seen in Figure 4.1. There are five agents representing energy sources. Agents 1, 7, 8, 9 and 10 stand for connection to the main grid, BUG, BESS, wind generator and PV farm respectively.

Moreover, agents 9 and 10 represent the renewable sources and their power generation is highly requested. Therefore, it is reasonable to use all the generated energy by them in every time step and to consider them as passive agents, that can not be controlled.

Besides them, the system consists of five agents numbered 2 to 6 that represent power loads. Similarly to renewable sources, they are considered to be non-controllable passive agents. Even though the agent 2 - Simris includes some elements of demand management, they will not be considered in this work due to their low power capacity in comparison with the BESS. Nevertheless, they might prove themselves to be very useful in other applications.
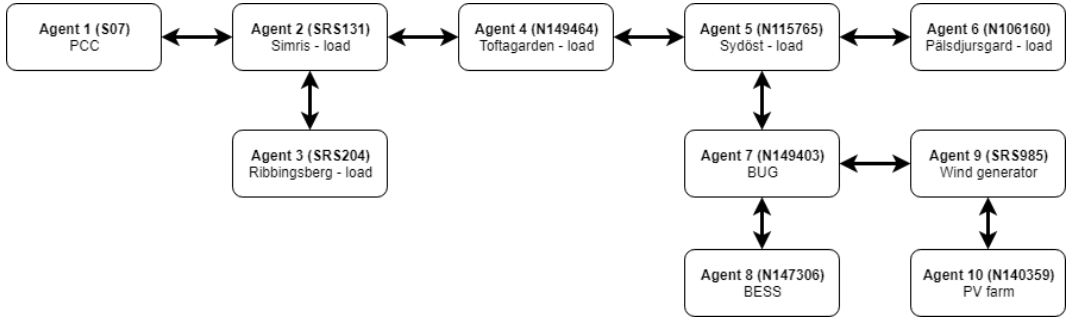
Figure 4.1: Agent representation of demonstration site situation

Hence, the created control uses only the power outputs of agent 1, 7 and 8 as the active contribution to the system. The power outputs of the other agents are taken as disturbances, that have to be covered by the active agents. The set of agents can be divided into two subsets,

$$P_A = \{P_1, \ P_7, \ P_8\},$$
$$P_P = \{P_2, \ P_3, \ P_4, \ P_5, \ P_6, \ P_9, \ P_{10}\}.$$

For the distributed MAS control, the communication between agents is possible in the way as it is shown in Figure 4.1. It is an example of topology communication architecture as it was explained in Section 2.2.3, each agent can communicate only with its direct physical neighbours.

All three active agents contain the information about the cost of the power that they can generate and based on the ratio between these costs, the energy mismatch of the network is distributed between active agents.

On the second control level, the MPC controller uses for the optimization of the distributed process information of the BESS SoC and set its price to be the most

convenient for the overall system. By the set of control parameters, the emphasis of the algorithm can be placed on the specific system features or used to solve the trade-off between them.

This process does not aim to supplement the distributed algorithm, rather it optimizes its operations by considering the BESS. The general design of the overall control is shown in Figure 4.2.
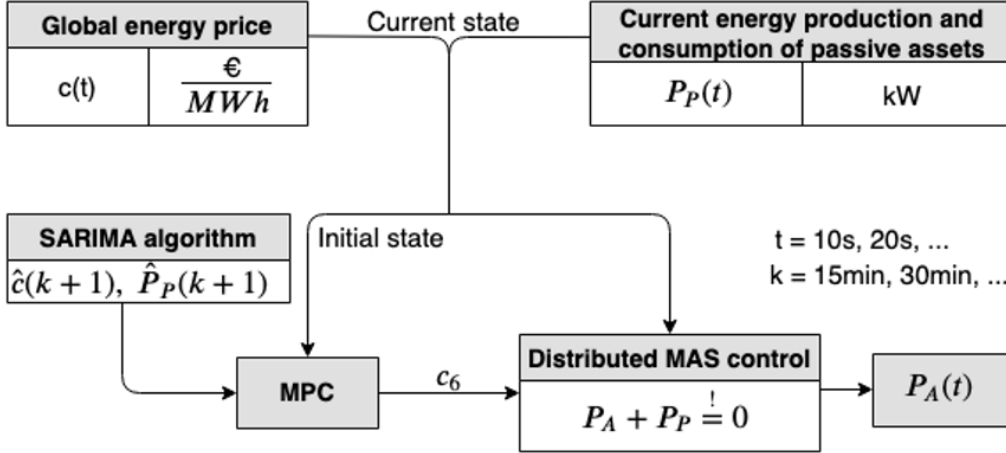
Figure 4.2: General structure of control algorithm

The distributed MAS control is executed every 10 seconds. The current data of power generation/demand of passive agents are summed up and cost function parameters are loaded to the individual active agents. Subsequently, by the distributed consensus algorithm the power mismatch of the passive agents is taken care of by optimal power distribution between the active agents.

For visualization in Figure 4.2, the individual cost parameters are summed up in the vector c,

$$c = \begin{bmatrix} a_1 \\ b_1 \\ a_7 \\ b_7 \\ a_8 \\ b_8 \end{bmatrix} = \begin{bmatrix} c_1 \\ c_2 \\ c_3 \\ c_4 \\ c_5 \\ c_6 \end{bmatrix}.$$

Moreover, every 15 minutes the cost function parameters of the BESS are set by the MPC controller and used for the period until the next MPC iteration. For the evaluation of the MPC, the cost function is built on current data and forecast future time-steps. After that, the cost function is minimized and the optimal control parameters are found.

4.2 Distributed MAS control

The consensus algorithm as a distributed MAS control solution is mentioned already in several articles [9, 17, 16]. In general, the overall balancing problem is formulated by equation (4.1),

$$\sum_i P_{G,i} + \sum_m P_{R,m} = -\sum_j P_{L,j}, \tag{4.1}$$

where the $\sum_i P_{G,i}$ represents all the overall generated power by conventional sources as well as by the BESS, the $\sum_m P_{R,m}$ symbolizes the power generated by renewable sources and finally, the $\sum_j P_{L,j}$ is the summation of the overall load demand. The total generated power is divided into these two groups because distributed renewable sources are considered as an uncontrollable input to the network.

The quadratic cost is assigned to each controllable source [16],

$$C_i(P_{G,i}) = \frac{1}{2} a_i (P_{G,i})^2 + b_i (P_{G,i}) + c_i \tag{4.2}$$

with a_i, b_i, c_i as cost parameters. By the distributed algorithm the summation of these prices should be minimized to set the optimal ratio of the power distribution between all active power sources,

$$min \quad \sum_i C_i. \tag{4.3}$$

To find the minimum value of this problem, the first derivation of all cost functions is needed,

$$r_i = a_i P_i + b_i. \tag{4.4}$$

Now, only the cooperation of all the agents on finding the common value of r is necessary. This process can be done in a centralised manner. Since the load, as well as the power generation from renewable sources, proved to be intermittent the advantages of distributed control such as control speed, reliability, and the control flexibility might be useful.

4.2.1 Weighted adjacency matrix

As was described in Section 2.2.3 the choice of the weighted adjacency matrix D of grid communication is crucial for the speed of convergence of the algorithm. The matrix D can not be designed completely randomly, all its elements must be non-negative and summation of each row equal to one. Therefore, the following equations (4.5) must hold,

$$D \cdot e = e, \ \ D^T \cdot e = e, \text{with } e = \begin{bmatrix} 1 \\ 1 \\ \vdots \\ 1 \end{bmatrix}. \tag{4.5}$$

Matrix D is designed in this way is called the doubly stochastic matrix. According to *Perron-Frobenius Lemma* [42], the eigenvalues of this matrix are less or equal to 1 with one eigenvalue 1 and the limit value of the D matrix in infinity can be computed by following equation,

$$J = \lim_{k \to \infty} D^k = \frac{ee^T}{n},$$ (4.6)

where n is the matrix dimension.

There are multiple approaches to how to get a weighted adjacency matrix for the power system. Since the communication links between individual agents are bidirectional, it makes sense to create matrix D which is symmetrical over the main diagonal, therefore $d_{ij} = d_{ji}$. These elements d_{ij} of the matrix D represent the coefficients of information exchange in the network. The elements on the main diagonal are then computed as a subtraction of all these elements in the row from one. By this approach, the sum condition is ensured.

The most conventional approach to set the coefficients in the network is called *Uniform method*. The elements of the D matrix are computed concerning the amount of nodes in the overall network. The *Uniform method* rule is summarized in following equation (4.7),

$$d_{ij} = \begin{cases} \frac{1}{n}, & j \in N_i, \\ 1 - \sum_{j \in N_i} \frac{1}{n}, & i = j, \\ 0, & \text{otherwise}, \end{cases}$$ (4.7)

where n is the amount of the nodes in the network. Even though the speed of the convergence might be a little bit improved by adapting the algorithm to the specific network, for this application it is sufficient. The simplicity of the application, as well as stability guarantee, are also important advantages.

The final D matrix for the system that is shown in Figure 4.1 is expressed like this

$$D = \begin{pmatrix} 0.9 & 0.1 & 0 & 0 & 0 & 0 & 0 & 0 & 0 & 0 \\ 0.1 & 0.7 & 0.1 & 0.1 & 0 & 0 & 0 & 0 & 0 & 0 \\ 0 & 0.1 & 0.9 & 0 & 0 & 0 & 0 & 0 & 0 & 0 \\ 0 & 0.1 & 0 & 0.8 & 0.1 & 0 & 0 & 0 & 0 & 0 \\ 0 & 0 & 0 & 0.1 & 0.7 & 0.1 & 0.1 & 0 & 0 & 0 \\ 0 & 0 & 0 & 0 & 0.1 & 0.9 & 0 & 0 & 0 & 0 \\ 0 & 0 & 0 & 0 & 0.1 & 0 & 0.7 & 0.1 & 0.1 & 0 \\ 0 & 0 & 0 & 0 & 0 & 0 & 0.1 & 0.9 & 0 & 0 \\ 0 & 0 & 0 & 0 & 0 & 0 & 0.1 & 0 & 0.8 & 0.1 \\ 0 & 0 & 0 & 0 & 0 & 0 & 0 & 0 & 0.1 & 0.9 \end{pmatrix}.$$ (4.8)

4.2.2 Multi-agent system control constraints

The real system is limited by the set of control constraints. Simple example of these limitations can be the fact that the energy can not be drawn out from the

BESS when its SoC drops under pre-set limit or the physically impossible process of charging the energy to the BUG.

In the consensus algorithm, all the constraints can be implemented with the same approach. When any limit of active agent is exceeded, its initial consensus value drops to zero and the produced power is set as a constant. By this adjustment the active agent is converted into the passive agent for this specific time-step, the power mismatch in a microgrid is recalculated and the consensus algorithm iteration process can continue.

The control constraints that are implemented into the algorithms can be seen in Table 4.1:

Microgrid component	Constraint	Value
Li-Ion BESS	energy capacity	333 kWh
	Minimal SoC	0.2
	Maximal SoC	0.9
	Maximal charge	1342.32 kW
	Maximal discharge	839.02 kW
BUG	Maximal power	350 kW
	Minimal power	0 kW

Table 4.1: Table of control constraints of MAS control

Moreover, supplying the generated energy from the microgrid to the main grid is not allowed in the case when the BESS is not fully charged. Thank to these settings, the system is not selling the generated energy in situations when the energy reserves are low. This precaution aims to prepare the microgrid for unexpected fault situations better.

4.2.3 Update rules

The consensus algorithm for optimal power dispatch, as suggested in [16, 17, 9] is expressed by the following three equations,

$$
\begin{aligned}
r_i[k+1] &= \sum_{j \in N_i} d_{ij} r_j[k] + \epsilon P_{D,i}[k], \\
P_i[k+1] &= \frac{r_i[k+1] - b_i}{a_i}, \\
P_{D,i}[k+1] &= \sum_{j \in N_i} d_{ij} \left(P_{D,j}[k] + (P_j[k+1] - P_j[k]) \right),
\end{aligned}
\tag{4.9}
$$

where the r_i stands for optimal derivative of the cost (4.4) for agent i, ϵ is the convergence step and $P_{D,i}$ refers to local estimate of power mismatch in the network, see [17]. Algorithm (4.9) aims to determine consensus on variable r to which all individual r_is converge. When there is no difference between r_is in the entire network, the algorithm terminates.

The rules (4.9) can be stated concisely in matrix form,

$$
\begin{aligned}
R[k+1] &= D \cdot R[k] + \epsilon P_D[k], \\
P[k+1] &= B \cdot R[k+1] + G, \\
P_D[k+1] &= D \cdot P_D[k] + D \cdot (P[k+1] - P[k]),
\end{aligned}
\tag{4.10}
$$

where variables r_i are arranged into a column vector R, as well as $P_{D,i}$ and P_i into P_D and P. The matrices B and G contain the relationship between cost parameters; in the case of matrix B, they are located on the main diagonal in the form of $\frac{1}{a_i}$ and G is a column vector with components $\frac{-b_i}{a_i}$.

Furthermore, the dynamics of the whole distributed system can be examined in the state-space representation. For that, the individual cost derivatives r_i and $P_{D,i}$ are taken as state variables. Therefore, the system matrix is defined by the following equation,

$$
\begin{bmatrix} R[k+1] \\ P_D[k+1] \end{bmatrix} = \begin{bmatrix} D & \epsilon I \\ DB(D-I) & D + \epsilon DB \end{bmatrix} \cdot \begin{bmatrix} R[k] \\ P_D[k] \end{bmatrix},
\tag{4.11}
$$

where I refers to the identity matrix. System (4.11) is found not to converge to a steady-state consensus on at least some connected graph topologies [1]. This can be elucidated by looking at the nominal system; (4.11) for $\epsilon = 0$; having system matrix

$$
\begin{bmatrix} D & 0 \\ DB(D-I) & D \end{bmatrix}.
\tag{4.12}
$$

The matrix (4.12) contains repeated eigenvalue set of matrix D and due to the *Perron-Frobenius Theorem* the matrix D has the largest eigenvalue equal to 1 and all other with magnitudes strictly less than that. The whole control can be seen in the schematic diagram in Figure 4.3.

For D to have a single eigenvalue equal to 1, the graph must contain a spanning tree. This is crucial for convergence of consensus algorithms. The $\epsilon-$disturbance generally *does not* vanish on the subspace pertaining to *both* 1 eigenvalues of (4.12). This subtle fact invalidates the logic based on the robustness of the consensus algorithm, as used in [16, 17, 9]. Namely, no $\epsilon > 0$ can generally be found small enough to ensure convergence.

4.2.4 Algorithm implementation

The necessary information for the algorithm implementation is the cost function parameters of agents 1, 7 and 8. Since that the costs of agent 1 and 7 depend linearly on the created power, the a coefficients are set very low, $a_1 = a_7 = 0.001$.

For the connection to the macrogrid, the real data are taken from the historical data of the official web-page of the *Nord pool* as it was introduced in the previous chapter.

For the back-up generator, the comparison with energy price from the main grid is used and BUG energy is assumed to be approximately 10 times more expensive.
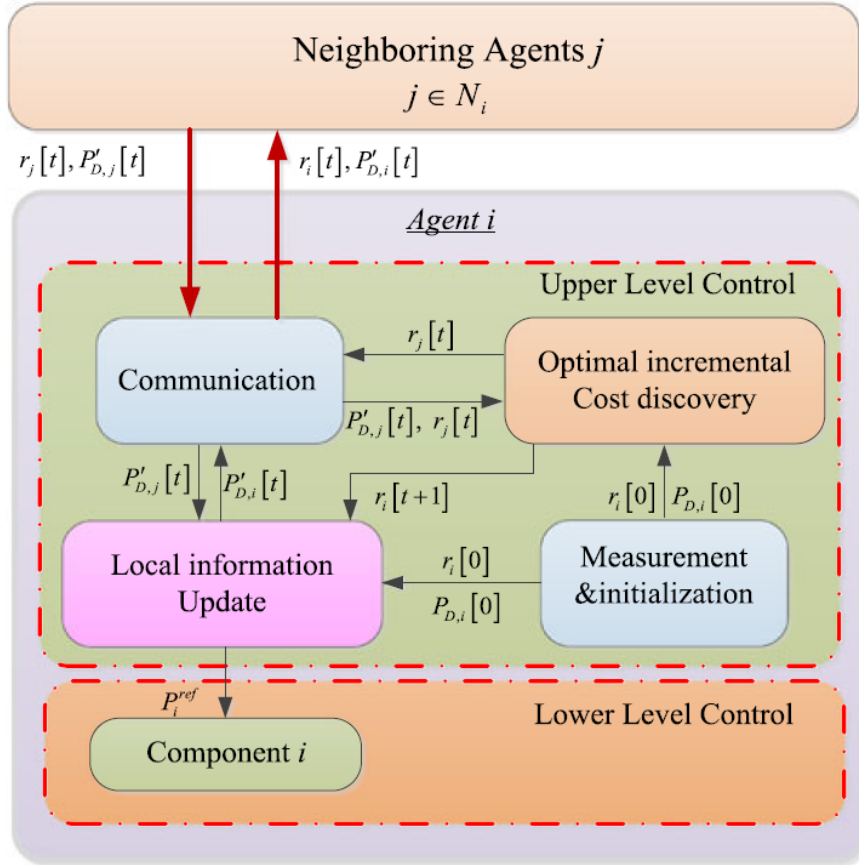
Figure 4.3: Schematic diagram of the distributed MAS control [9]

Therefore, the cost parameter of BUG is set to ten times higher value for the whole simulation, $b7 = 10 \cdot b_1$. This should not influence the simulation because the BUG is meant to be used only occasionally, in moments when microgrid control collapses. This is not the topic of this work and it will not be further examined.

Now, we have two cost function parameters of the BESS which can be used to influence the ratio of the power distribution. Unfortunately, optimizing of two parameters with quite tightly bounded relation can be very complex and computationally demanding. Moreover, the a_8 parameter is only setting the sensitivity of the final ratio on the related b parameter. With the unlimited precision of parameter setting, it can be considered constant. Therefore, the parameter a is set to the following value, $a_8 = 0.1$.

Convergence issues of the cooperative algorithm mentioned in the previous section motivate the development of a modified control protocol which does not suffer from these problems.

At first, the solution by rescaling the whole lower part of the system matrix to shrink the Gerschgorin's disks of the respective eigenvalues inside the unit circle was tried. Unfortunately, this solution solved the stability problem, but also drastically changed the whole dynamics of the system.

Other tested solution was the attempt to change the matrix D in the way that it would solve the stability issues. Unfortunately, the D matrix must fulfil the requirements for the stochastic matrix and therefore it can not be changed in the way in which $D + \epsilon DB$ is not doubly stochastic as well.

The solution was found eventually [1]. By scaling the lower right block of the system matrix (4.11) by a positive scalar factor $\alpha < 1$, the system (4.15) converges to steady-state consensus in r_is. The single agent's update rules are given as,

$$r_i[k+1] = \sum_{j \in N_i} d_{ij} r_j[k] + \epsilon P_{D,i}[k],$$

$$P_i[k+1] = \frac{r_i[k+1] - b_i}{a_i}, \tag{4.13}$$

$$P_{D,i}[k+1] = \sum_{j \in N_i} d_{ij} \left(\alpha P_{D,j}[k] + (P_j[k+1] - P_j[k]) \right),$$

for $0 < \alpha < 1$. In matrix form this reads,

$$R[k+1] = D \cdot R[k] + \epsilon P_D[k],$$

$$P[k+1] = B \cdot R[k+1] + G, \tag{4.14}$$

$$P_D[k+1] = \alpha D \cdot P_D[k] + D \cdot (P[k+1] - P[k]).$$

The adjusted system can be represented by the following state-space dynamics,

$$\begin{bmatrix} R[k+1] \\ P_D[k+1] \end{bmatrix} = \begin{bmatrix} D & \epsilon I \\ DB(D-I) & \alpha D + \epsilon DB \end{bmatrix} \cdot \begin{bmatrix} R[k] \\ P_D[k] \end{bmatrix}. \tag{4.15}$$

Theorem 1 (Proposed algorithm). *For any $0 < \alpha < 1$ the system (4.15) converges to the span $\begin{bmatrix} \underline{1}^T & 0 \end{bmatrix}^T$ on arbitrary graph topologies containing a spanning tree, given $\epsilon > 0$ is sufficiently small.*

Proof. For $0 < \alpha < 1$, the nominal system matrix

$$A_{nom} = \begin{bmatrix} D & 0 \\ DB(D-I) & \alpha D \end{bmatrix} \tag{4.16}$$

has a single eigenvalue 1 with eigenvector $\begin{bmatrix} \underline{1}^T & 0 \end{bmatrix}^T$; all other eigenvalues of (4.16) have absolute value strictly less than 1. Hence, the second-largest nominal system eigenvalue satisfies $\overline{\lambda_{<1}}(A_{nom}) = max(\overline{\lambda_{<1}}(D), \alpha) < 1$.

The $\epsilon-$perturbation vanishes on span $\begin{bmatrix} \underline{1}^T & 0 \end{bmatrix}^T$ for $\forall \epsilon > 0$

$$\epsilon A_d \begin{bmatrix} \underline{1} \\ 0 \end{bmatrix} := \epsilon \begin{bmatrix} 0 & I \\ 0 & DB \end{bmatrix} \begin{bmatrix} \underline{1} \\ 0 \end{bmatrix} = 0. \tag{4.17}$$

For convergences of the original system (4.15) to the span $\begin{bmatrix} \underline{1}^T & 0 \end{bmatrix}^T$ the second largest eigenvalue of the system (4.15) needs to satisfy

$$|\overline{\lambda_{<1}}(A_{nom} + \epsilon A_d)| < 1. \tag{4.18}$$

As one has,

$$|\overline{\lambda_{<1}}(A_{nom} + \epsilon A_d)| \leq |\overline{\lambda_{<1}}(A_{nom})| + \epsilon|\overline{\lambda}(A_d)| \tag{4.19}$$

(4.18) is certainly satisfied for

$$\epsilon < \frac{1 - |\overline{\lambda_{<1}}(A_{nom})|}{|\overline{\lambda}(A_d)|}, \tag{4.20}$$

giving an upper bound on ϵ to fulfil the condition (4.18). □

The obtained system has the same properties as a leaderless consensus algorithm, according to [7]. The final iterated value of the consensus variable r depends only on the initial values of r_is. Since the amount of produced or used power is known, this information can be distributed through the network to compute the power mismatch in the grid. This is required for determining the optimum controller's initial values as well as the cost functions.

This is different from the protocol described in [16, 17, 9]. A few hundred iterations are needed for finding the consensus value but the required distribution of the data through the network is done very quickly. That is a price to pay for having a stabilized system with perfectly deterministic behaviour. The algorithm retains all the advantages of distributed solutions such as lower complexity, reliability, and security and it is guaranteed to converge on arbitrary graph topologies containing a spanning tree.

Moreover, the distributed multi-agent system (MAS) consensus algorithm can also be initialized with partially known data. That speeds up the initial reaction of the controller, which might be useful in case of a rapidly changing environment typical for RES microgrids. The iteration process of the consensus algorithm on consensus values r can be seen in Figure 4.4.

4.3 Model predictive control

The second level of control is embedded by the centralised MPC controller to minimize the costs of energy imported from the macrogrid (negative number stands for selling energy) and optimize the BESS SoC by keeping it on a 50% level.

As it was explained in Section 2.3, this type of controller requires a model of the system and prediction of the system disturbances, in this case in the form of microgrid power mismatch and future global energy price.

Besides that, the cost function needs to be rightly set and weighted to find the optimal trade-off between both observed values. It has to also take all kinds of the restriction and limitation of the system into consideration.
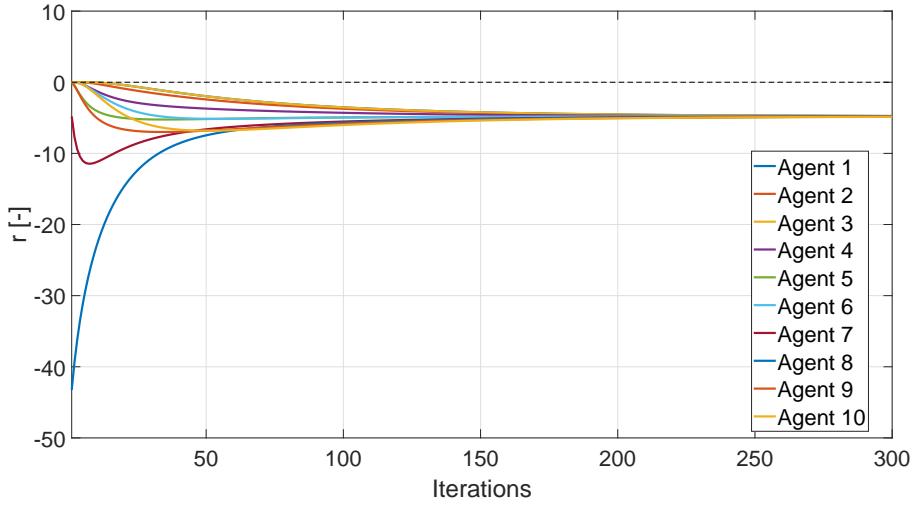
Figure 4.4: Consensus algorithm iteration for one time step

As was said in the introduction to this chapter, the MPC control is executed once every 15 minutes and it sets the cost function parameters of the BESS for the following 15 minutes. Hence, the 90 cycles of the first layer control are performed during one step of the MPC controller.

4.3.1 Designed model

Naturally, the most relevant variable of the BESS is its SoC. Nevertheless, for the computation reasons the energy with which is the battery pack charged will be used as a state variable. Thanks to that the state space equation stays significantly less complex. With the knowledge of the maximum energy capacity of the BESS, it is simple to convert this value to needed SoC. The battery energy is held in kWh.

The state equation of the BESS energy can be expressed by equation (4.21),

$$x[k+1] = x[k] - \frac{r - b_8}{4a_8}, \tag{4.21}$$

where r is the optimum cost that was found by consensus algorithm and a_8 with b_8 are cost parameters of agent 8 - BESS. Since the MPC operates only every 15 minutes the new capacity is computed as if the power distribution between individual agents stays the same as in the time-step k for the whole time. The factor of $\frac{1}{4}$ in this equation is caused by the recalculation of the used energy to kWh.

The calculation of the variable r is done from the known mismatch in the network and active agent's cost function parameters. In our specific case, it can be written in the following manner,

$$r = \frac{-s + \frac{b1}{a1} + \frac{b7}{a7} + \frac{b8}{a8}}{\frac{1}{a1} + \frac{1}{a7} + \frac{1}{a8}}, \tag{4.22}$$

where s is the network power mismatch and parameters a and b refer to agent 1 - PCC, agent 7 - BUG and agent 8 - BESS based on their identification numbers. In case that the s is not known for the computed time step, its estimation $\hat{s}$ might be used.

The probability of the real power distribution staying completely constant for 15 minutes is very low. After all, there are 90-time steps in which the distribution ratio can be changed. This model configuration is given an estimate that is showing what capacity would be available in the next MPC time step.

With consideration of all these model settings, the state equation (4.21) has two uncontrollable inputs s and b_1 and controllable b_8 which is used for MPC control.

4.3.2 Data forecast

To obtain the necessary data forecast the regression analysis on provided data is utilized. Both of the predicted data sequences, energy prices, and power mismatch, show high dependency on the time of day when they were measured. Unfortunately, that is not the only relationship among data that can be observed. From the measured datasets, it is clear that the individual days are not completely independent.

Firstly, the Gaussian process regression model is used to estimate future data. Even though some dependencies between data are preserved, the predicted model stayed constant for all days and the amplitudes of the data vector are very different. Therefore, this estimated model did not correspond well with reality.

The non-stationarity between days had to been added to the model. For this problem, the typical regression solution of econometrics is used. The seasonal autoregressive integrated moving average (SARIMA) model estimates the relationships among variables by autoregressive method, it takes defined previous known data to forecast the future ones.

The name of the algorithm is composed of three parts. Autoregression represents the fact that the model is finding dependencies between previously known or own lagged data. The word integrated stands for the fact, that the individual time series values are converted into the differences between the two following time steps. Thanks to that, the time series becomes stationary.

Finally, the moving average refers to the relationship between regression error of the previous data and the individual observations by computing their linear combination. The computed variable is then minimized by any minimizing algorithm. In the following implementation, the minimized mean square error (MMSE) algorithm is used.

Moreover, the model adaptation SARIMA can add the pattern between data that repeats itself. In this case, the repeating pattern every 96-time steps (one day) can be easily observed on the measured data.

After setting up the described model, the prediction results are very satisfying in comparison with Gaussian process model. The prediction of the one full day after learning on 7 days data can be seen in Figure 4.5 also with a 95% forecast probability of the MMSE algorithm.

The SARIMA model is implemented by *MATLAB* build-in function *arima* [50] and its parameters are chosen by *Econometric Modeler App.* This application is a part of the same program and provides to a user a way to choose the right settings for given data.
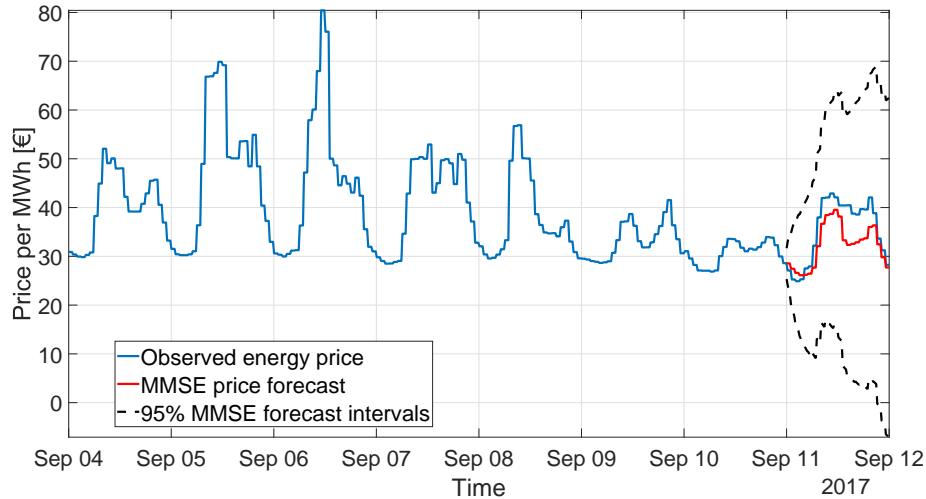
Figure 4.5: One-day prediction of global energy prices by an estimated SARIMA model

The performance of the prediction algorithm shows quality approximation all over predicted 96-time steps. Taking into account the fact, that the MPC predictive horizon will not be that long in the implemented program, the behaviour of the forecast algorithm is completely sufficient.

The graph of real data, one step prediction (15 minutes) and 24 steps prediction (6 hours) on the dataset of 5 days between 11.9.2017 and 16.9.2017 for both microgrid mismatch and global energy prices are shown in Figures 4.6 and 4.7, respectively.

The performance of short, one step prediction is very functional and the predictions are tracking the real data very tightly. It can be seen that the long prediction, as 6 hours prediction is, reacts late to large steps in the real data curves. In the case of power mismatch in the microgrid, the long prediction shows obvious drawbacks and the performance of the MPC algorithm could be strongly influenced by inaccurate prediction. On the other hand, in the case of global energy price data, the real data curve is quite seasonal and significantly more predictable than power mismatch. That is the reason why this long prediction also tracks the reality better and can be used in the algorithm deployment.
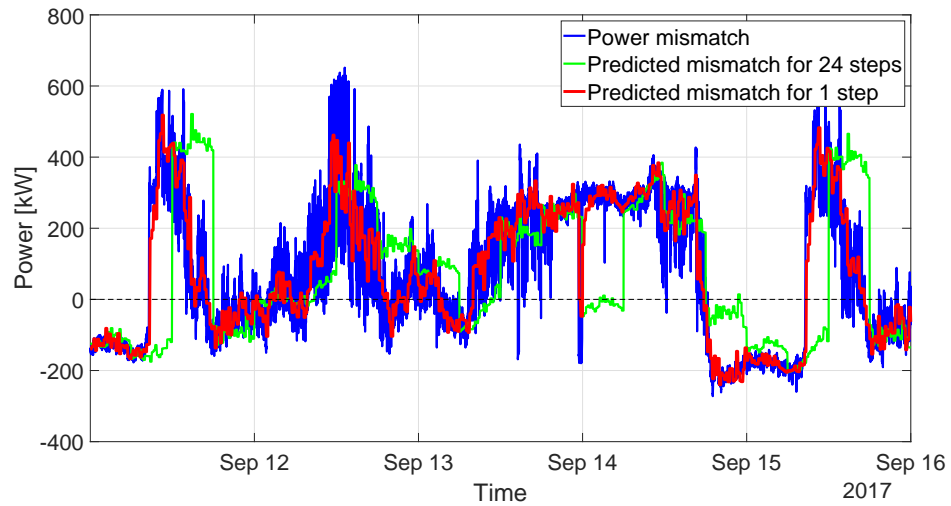
Figure 4.6: Prediction of microgrid mismatch compared with real data on one week dataset
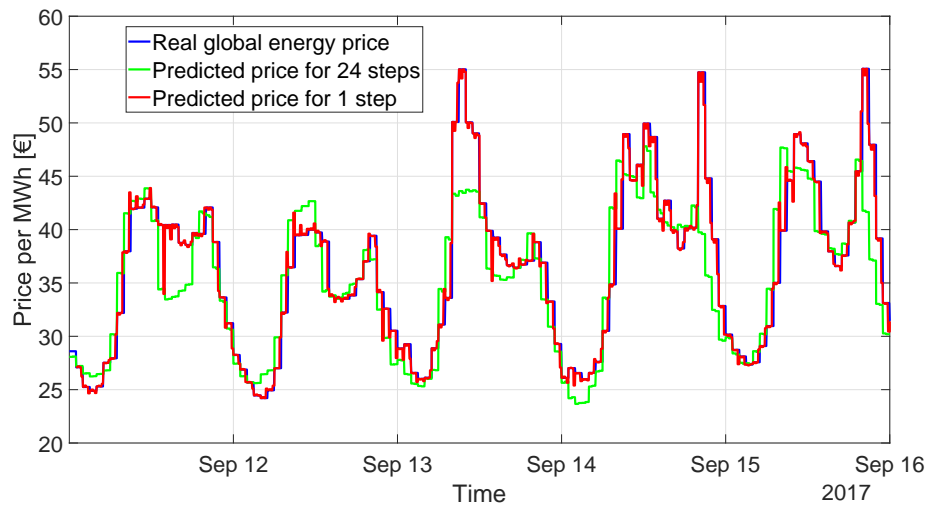
Figure 4.7: Prediction of global energy price compared with real data on one week dataset

4.3.3 Cost function

As was mentioned in Section 2.3.1 the right selection of the cost function and its parameters by network operator is crucial for providing the required control performance.

The cost function in the controller implementation is chosen in a little bit different style that was presented in equation (2.5). Implemented cost function is in the following form (4.23),

$$V(b_8) = Q \sum_{k=1}^{T_p} \left[\tfrac{E}{2} - \hat{x}[k](b_8) \right]^2 + R \sum_{t=0}^{T_p-1} \left[\hat{b}_1[t] \cdot \tfrac{r[t](b_8) - \hat{b}_1[t]}{a_1} \right], \qquad (4.23)$$

where E stands for maximal energy that can be stored in the BESS. In the computation of the current time-step of the second term, the real system state $x[k]$ is used instead of its prediction $\hat{x}[k]$ similarly as the real power price coefficient b_1. In the following prediction steps, the system variable prediction is computed by using data forecast.

In the implementation, the control horizon is set to the same value as the predictive horizon. This decision is made due to the fact, that the future evolution of this specific system continues on a trajectory that is penalized according to future states and control efforts necessary for moving between them.

The cost function is the subject of minimization of dependency on only one variable. By this simplification, the whole process of minimization becomes computationally easier, less complex and faster.

The first part of the cost function sets the price of distance of the BESS charged energy from 50% of battery capacity. With every deviation by which the stored energy differs from the middle of capacity, the cost of this part of the equation grows quadratically. This value is multiplied by its coefficient Q.

The second part of the equation expresses the price of power delivered to the microgrid through the PCC and it is weighted by coefficient R. This equation term is linear because of the possibility of supplying energy back to the main grid which is expressed by its negative cost. With the right settings of two coefficients R and Q, the importance of each phenomenon is set and the trade-off between them is optimally balanced.

When the function reaches a steady-state, the optimal values of b_8 for future T_p steps are found. From this created control sequence the first control input is taken and applied to the system. The rest is discarded and the whole process is repeated in the following time step.

4.3.4 Prediction constraints

For the quality and meaningful prediction of the system's future behaviour, it is necessary to constrain the system state into which the model can get in the future steps. Since the price of energy from the main grid is not limited, the second term of cost function (4.23) can be minimized as it is.

On the other hand, that is not the case for its first term. The limitations of BESS are presented in the previous Table 4.1 and it would not make sense for the MPC algorithm to take the future states with SoC outside of these limits into consideration.

5 Exemplary Results

In the last part of the thesis, the performance of the implemented control algorithm is evaluated on measured data. The parameters are chosen for economical evaluation as well as for the measurement of the BESS utilization.

The control results are simulated in several tests. First, the control algorithm results are compared depending on the setting of the control parameters, the ratio between MPC cost function Q and R and the length of the predictive horizon. Each control settings is used on data from multiple days to validate its repeatability.

In the second part, the simulation results of the proposed algorithm are shown compared with the reference control algorithm as well as with the situation of microgrid without distributed ESS.

5.1 Evaluation metrics

To provide a complex evaluation of the algorithm performance, multiple independent evaluation metrics are used to ensure objectivity. All observed measured features can be divided into 3 groups, metrics considering economical aspects of the simulated results, metric regarding power exchange with the main grid and metric of the BESS performance.

5.1.1 Economical metrics

The evaluation of the control algorithm based on the economical results can be considered as the most important aspect for its theoretical future deployment. Algorithm, that confirms its benefit by lowering of total variable costs provides to the system authorities strong reasoning for its utilization in the microgrid as well as the expected profitability of the project.

In the upcoming simulations, the total cost of the energy drawn from the main grid will be computed. Similarly, the assumption of selling energy back to the macrogrid by the same actual price is made and total revenues from energy trades are estimated. The earnings made by selling energy are taken as negative costs.

At the end of the test, these two values are summed up and the total flexible cost of the control algorithm use is determined. For the sake of better comparison between multiple tests of different lengths, the average cost of energy per day is also added.

Due to the expected high dependency of total costs on power mismatch during the test period, the comparison with other control algorithms is executed on the same

data. Therefore, the simulation of the control without distributed ESSs is carried out as well as the reference control presented in Section 3.4.

The differences between these two approaches are described by absolute cost reduction in Euros and relative cost reduction. Analysis of these value is the most relevant for the assessment of the suggested algorithm functionality.

5.1.2 Power exchange metrics

The second group of used measuring metrics takes the exchange of energy with the main grid through the PCC into consideration. The total amount of energy drawn from the main grid in kWh, as well as the total quantity of created energy that is supplied to the macrogrid, are measured.

5.1.3 BESS metrics

The last category of proposed measuring metrics evaluates the performance of the algorithm regarding processes on the BESS. The battery processes can be examined for several different reasons.

In case of including of BESS into microgrid, it is reasonable to utilize it whenever the conditions are appropriate. Deployment of BESS represents a quite large fixed cost of the system which has to be taken care of by revenues of the system. In the case of intermittent usage of the BESS, the expense of integrating it into the system might become unreasonable.

This BESS feature can be observed through multiple parameters. During the tests, the charged and discharged energy to the batteries are measured and the equivalent full battery cycles are computed from the individual charging and discharging sequences. The amount of full equivalent cycles is then averaged to find comparable value of one-day utilization.

Another important aspect of BESS is the process of ageing. Even though the process of ageing of lithium-ion (Li-ion) batteries is unavoidable, some processes are more convenient for the battery pack than others. For example, the often cycling of the batteries as well as high charging and discharging currents are strongly unwanted.

As can be seen, the required utilization of Li-ion batteries is not straight forward and the final decision must be done by a microgrid operator.

5.2 Simulation results

All simulated tests are done on the previously described microgrid solution data using a suggested control algorithm with different settings of control parameters. The control performance is tested on multiple day sequences from measured data.

For the successful use of the SARIMA models introduced in Section 4.3.2, previously known measured values are required. Therefore, the first week is not used for testing and due to that, at least seven days are always used for training of SARIMA model.

For the possibility of result comparison, the simulation of the system with the reference control, as well as the simulation of the system without BESS, are executed. The total costs of the system controlled by these algorithms are measured.

During all simulations shown in this chapter, the following conventions are used. Energy drawn from the main grid is taken as positive and energy supplied to the main grid as negative. The same convention also applies to powers. In the case of energy prices, the positive values represent bought energy and negative sold one. Lastly, the comparison done with the reference control in positive values shows that the suggested control algorithm is more advantageous.

5.2.1 Control parameters settings

Necessary control parameters, the ratio between parameters of the MPC cost function Q and R, as well as the predictive horizon h, are set based on performed tests.

Q/R ratio

The same control algorithm settings are applied on multiple control settings with only difference in the ratio of Q and R parameters. The test is performed twice on two different datasets to ensure the correct settings.

Simulation 1 - 3 days between 18.9.2017 and 20.9.2017   The results of simulation for both reference systems are the following:

- System without BESS

$$C_1 = -32.23 \text{ €}$$

- Reference control

$$C_2 = -33.65 \text{ €}$$

#	MPC settings			Power exchange results				
	h	Q	R	$E_{tot,in}[kWh]$	$E_{tot,out}[kWh]$	$C_{tot,in}[€]$	$C_{tot,out}[€]$	$C_{tot}[€]$
1	24	5	1	4391.29	-5274.90	173.02	-216.89	-43.88
2	24	1	1	4377.94	-5337.82	171.59	-219.97	-48.38
3	**24**	**1**	**2**	**4387.00**	**-5347.51**	**171.57**	**-220.42**	**-48.85**
4	24	1	3	4366.48	-5326.92	170.77	-219.44	-48.67
5	24	1	5	4379.32	-5339.85	171.44	-220.07	-48.63

Table 5.1: Table showing MPC settings and power exchange results of Simulation 1

The performance of the implemented algorithm can be seen in Tables 5.1 and 5.2. The columns of Table 5.1 refer to test number, predictive horizon h, control parameter Q, control parameter R, total energy drawn by the microgrid $E_{tot,in}$,

#	BESS results				Comparison			
	$E_{tot,char}[kWh]$	$E_{tot,dis}[kWh]$	EFC	$\overline{EFC}$	$C_{r,1}[\text{€}]$	$C_{r,1}[\%]$	$C_{r,2}[\text{€}]$	$C_{r,2}[\%]$
1	2130.41	-2159.08	9.14	3.05	11.65	36.15	10.23	30.40
2	1954.27	-2053.07	8.38	2.79	16.15	50.10	14.73	43.76
3	**1932.32**	**-2031.72**	**8.29**	**2.76**	**16.62**	**51.56**	**15.20**	**45.16**
4	1920.17	-2019.52	8.24	2.75	16.44	51.01	15.02	44.64
5	1724.44	-1823.83	7.39	2.47	16.41	50.90	15.02	44.52

Table 5.2: Table showing BESS processes results and comparison with reference algorithms of Simulation 1

supplied to the main grid $E_{tot,out}$, total cost of drawn energy $C_{tot,in}$, total cost of supplied energy $C_{tot,out}$ and summation of these two costs (left to right).

The individual tests are refereed by the same number in Table 5.2. The other columns represent total energy deposited into the BESS $E_{tot,char}$, total energy discharged from BESS $E_{tot,dis}$, amount of equivalent full cycles EFC, day-average of equivalent full battery cycles, comparison with the first reference control in Euros and in percentage $C_{r,1}$ and same comparison with second reference architecture $C_{r,2}$ (left to right).

Based on the Simulation 1 results, the control settings in test 3 turned out to be the one with the highest relative cost comparison. This setting is used in the full test at the end of this chapter. It can be also observed that with the growing emphasis on the BESS SoC the utilization of BESS also increases. This fact can be seen in the part of Table 5.2 BESS results. It is worth noting that the energy exchange with the main grid does not depend on this feature.

To make sure that the selected parameters are providing the most advantageous control, a similar test is done for the next 3 days.

Simulation 2 - 3 days between 21.9.2017 and 23.9.2017   The results of simulation of both reference systems are the following:

- System without BESS
$$C_1 = 383.00 \text{ €}$$

- Reference control
$$C_2 = 377.86 \text{ €}$$

The performance of the implemented algorithm can be seen in Tables 5.3 and 5.4.

#	MPC settings			Power exchange results				
	h	Q	R	$E_{tot,in}[kWh]$	$E_{tot,out}[kWh]$	$C_{tot,in}[€]$	$C_{tot,out}[€]$	$C_{tot}[€]$
6	24	1	1	10260.62	-206.54	379.31	-9.29	370.02
7	**24**	**1**	**2**	**10195.22**	**-161.25**	**376.29**	**-6.92**	**369.37**
8	24	1	3	10243.15	-232.69	380.17	-10.21	369.97

Table 5.3: Table showing MPC settings and power exchange results of Simulation 2

#	BESS results				Comparison			
	$E_{tot,char}[kWh]$	$E_{tot,dis}[kWh]$	EFC	$\overline{EFC}$	$C_{r,1}[€]$	$C_{r,1}[\%]$	$C_{r,2}[€]$	$C_{r,2}[\%]$
6	3748.90	-3753.24	16.08	5.36	12.99	3.39	7.84	2.08
7	**3943.91**	**-3966.76**	**16.91**	**5.64**	**13.64**	**3.56**	**8.49**	**2.25**
8	3638.75	-3683.22	15.61	5.20	13.04	3.40	7.89	2.09

Table 5.4: Table showing BESS processes results and comparison with reference algorithms of Simulation 2

Also, the results from the Simulation 2 show that the most convenient ratio between Q and R is 1:2. It would be possible to find the optimal Q/R ratio even more precisely by executing other tests with values close to the chosen ratio. However, the results do not differ that much from each other so the small adjustment of the ratio would not have appreciable added value.

The dependency of the BESS utilization on Q parameter is not that obvious in results from the Simulation 2, which can be caused by inaccuracies of individual final values of distributed MAS system iterations.

It is also very convenient that during these 3 days the production of distributed generators is lower than in the case of Simulation 1 and the total cost of the system is also quite large. The fact that the best results are once again generated by simulation with this Q/R ratio, represents very useful observation about the microgrid system. The mentioned Q/R ratio will be used from now on.

Predictive horizon h

The optimal predictive horizon h is found similarly. Unfortunately, the tests of the predictive horizon turn out to be affected by the prediction error. Therefore, the longer simulations are chosen to distribute the error between more program iterations and to find the optimal predictive horizon value.

Same as before, two tests are executed on two seven day-long datasets in the second and third week of the measured data.

Simulation 3 - 7 days between 18.9.2017 and 25.9.2017   The results of simulation for both reference systems are the following:

- System without BESS
$$C_1 = 334.07 \ \text{\euro}$$

- Reference control
$$C_2 = 329.49 \ \text{\euro}$$

The performance of the implemented algorithm can be seen in Tables 5.5 and 5.6.

#	MPC settings			Power exchange results				
	h	Q	R	$E_{tot,in}[kWh]$	$E_{tot,out}[kWh]$	$C_{tot,in}[\text{\euro}]$	$C_{tot,out}[\text{\euro}]$	$C_{tot}[\text{\euro}]$
9	3	1	2	15369.77	-6410.57	561.11	-254.91	306.20
10	**4**	**1**	**2**	**15414.75**	**-6455.55**	**562.58**	**-256.80**	**305.78**
11	5	1	2	15390.76	-6431.54	561.59	-255.75	305.84
12	8	1	2	15366.52	-6407.27	561.04	-254.63	306.40
13	12	1	2	15522.10	-6562.91	570.49	-262.47	308.02

Table 5.5: Table showing MPC settings and power exchange results of Simulation 3

#	BESS results				Comparison			
	$E_{tot,char}[kWh]$	$E_{tot,dis}[kWh]$	EFC	$\overline{EFC}$	$C_{r,1}[\text{\euro}]$	$C_{r,1}[\%]$	$C_{r,2}[\text{\euro}]$	$C_{r,2}[\%]$
9	5109.52	-4976.33	21.35	3.05	27.87	8.34	23.09	7.01
10	**5487.90**	**-5354.71**	**22.97**	**3.28**	**28.29**	**8.47**	**23.71**	**7.20**
11	5351.70	-5218.50	22.39	3.20	28.23	8.45	23.65	7.18
12	5719.19	-5585.99	23.96	3.42	27.67	8.28	23.09	7.01
13	5704.23	-5571.04	23.90	3.41	26.06	7.80	21.47	6.52

Table 5.6: Table showing BESS processes results and comparison with reference algorithms of Simulation 3

Simulation 4 - 7 days between 25.9.2017 and 2.10.2017   The results of simulation of both reference systems are the following:

- System without BESS
$$C_1 = -336.72 \text{ €}$$

- Reference control
$$C_2 = -338.90 \text{ €}$$

The performance of the implemented algorithm can be seen in Tables 5.7 and 5.8.

#	MPC settings			Power exchange results				
	h	Q	R	$E_{tot,in}[kWh]$	$E_{tot,out}[kWh]$	$C_{tot,in}[€]$	$C_{tot,out}[€]$	$C_{tot}[€]$
14	4	1	2	3558.68	-13686.14	112.77	-455.10	-342.34
15	**5**	**1**	**2**	**3572.31**	**-13696.30**	**113.19**	**-455.61**	**-342.41**
16	6	1	2	3969.89	-14076.84	125.76	-467.16	-341.40
17	8	1	2	3585.21	-13681.16	113.62	-455.08	-341.47

Table 5.7: Table showing MPC settings and power exchange results of Simulation 4

#	BESS results				Comparison			
	$E_{tot,char}[kWh]$	$E_{tot,dis}[kWh]$	EFC	$\overline{EFC}$	$C_{r,1}[€]$	$C_{r,1}[\%]$	$C_{r,2}[€]$	$C_{r,2}[\%]$
14	2601.98	-2700.25	11.16	1.59	5.62	1.67	3.44	1.02
15	**2653.97**	**-2749.05**	**11.39**	**1.63**	**5.69**	**1.69**	**3.51**	**1.04**
16	2533.37	-2612.70	10.87	1.55	4.68	1.39	2.50	0.74
17	2673.59	-2742.90	11.47	1.64	4.75	1.41	2.57	0.76

Table 5.8: Table showing BESS processes results and comparison with reference algorithms of Simulation 4

In comparison with previous simulation to set Q/R ratio, these two tests for predictive horizon did not come up with the same optimal value. Unlike the ratio, the predictive horizon has to be set as an integer. In Simulation 3 the optimal predictive horizon turned out to be equal to 4, in Simulation 4 h is equal to 5. Therefore, both of them will be used in the future simulation of the whole dataset. On the other hand, the relative cost reductions are very similar for both predictive horizon settings so this adjustment is not expected to change the results significantly.

The found values correspond with prediction time 1 hour and 1 hour and 15 minutes respectively. The fact that the optimality is found in such a short predictive horizon can be considered very convenient because with longer predictive horizon the MPC cost function starts to be quite complex and its minimization very computationally demanding.

It should be noted that the utilization of BESS is growing with longer prediction. Also, it is evident that the algorithm brings significant cost reduction when the energy production of the renewable sources in the microgrid is lower than energy demand for most of the time.

5.2.2 Simulation of complete data

Finally, the long-time period of 21 days between 11.9.2017 and 2.10.2017 is simulated with the previously found ratio $Q/R = 1 : 2$ and multiple predictive horizons. Once again, the results of simulation of both reference systems are the following:

- System without BESS

$$C_1 = -580.60 \text{ €}$$

- Reference control

$$C_2 = -599.88 \text{ €}$$

The final results can be seen in Tables 5.9 and 5.10.

#	MPC settings			Power exchange results				
	h	Q	R	$E_{tot,in}[kWh]$	$E_{tot,out}[kWh]$	$C_{tot,in}[€]$	$C_{tot,out}[€]$	$C_{tot}[€]$
17	3	1	2	25014.99	-40496.07	873.06	-1506.98	-633.92
18	**4**	**1**	**2**	**25131.73**	**-40613.60**	**868.55**	**-1502.93**	**-634.38**
19	5	1	2	25143.78	-40624.68	874.08	-1507.48	-633.40
20	6	1	2	25445.41	-40926.99	884.32	-1517.01	-632.69

Table 5.9: Table showing MPC settings and power exchange results of complete simulation

#	BESS results				Comparison			
	$E_{tot,char}[kWh]$	$E_{tot,dis}[kWh]$	EFC	$\overline{EFC}$	$C_{r,1}[€]$	$C_{r,1}[\%]$	$C_{r,2}[€]$	$C_{r,2}[\%]$
17	10457.00	-10555.42	44.86	2.14	53.31	9.18	34.04	5.67
18	**10050.65**	**-10149.81**	**43.12**	**2.05**	**53.77**	**9.26**	**34.5**	**5.75**
19	10290.51	-10388.76	44.15	2.10	52.80	9.10	33.52	5.59
20	10228.71	-10327.54	43.88	2.01	52.01	8.97	32.81	5.47

Table 5.10: Table showing BESS processes results and comparison with reference algorithms of complete simulation

From the measured data, it is evident that during this period the distributed generators are producing significant amount of energy. Despite the unfavourable conditions of the microgrid, the algorithm proved to be useful with relative cost reduction of approximately 9% and 5.75% compared to the reference system without BESS and reference control system, respectively.

In average, the utilization of the BESS is relatively high. With two full equivalent full cycles per day, the installation of BESS into the microgrid is justified. With the cost reduction, roughly 60 € in only one month promises returns on initial investment into battery technology.

The cost reduction of approximately 40 € per month compared to the reference control architecture shows that the control algorithms of microgrid network can provide a very interesting method of cost reduction or even revenue creation for the deployed microgrids.

6 Conclusion

The main aim of this thesis was to design a multi-agent model predictive control algorithm for microgrid architectures that would optimize its energy management.

The thesis fulfilled all the assigned tasks. After the general introduction to the topic, the current state-of-the-art microgrid concept as an energy grid solution is given in detail. Subsequently, the structure of common control strategies for microgrids as well as a model predictive control concept are presented.

In the second half of the thesis, the specific use case in southern Sweden is described, completed by the description of pre-processing methods applied to the measured data. Besides that, the reference control architecture for a representative comparison of the designed control results is presented.

In Chapter 4 the designed control architecture was presented. The control algorithm was implemented in two levels to maximize the utilization of two control approaches distributed MAS control and MPC.

The consensus algorithm is implemented as a type of distributed MAS control. This algorithm ensures the power balance in the microgrid based on power distribution between active nodes that represent controllable energy sources. The optimal ratio is found, based on the minimum total cost of the generated energy that is determined iteratively by communication of the consensus variable between individual agents.

On the other hand, the MPC control is aiming to set the parameters of the BESS cost function to provide optimal economical results valid for the simulation time horizon. The future states are forecast using SARIMA model prediction and the MPC cost function puts into relation the cost of future states of BESS with the cost of future energy exchange with the main grid. After then, the resulting equation is minimized with respect to BESS cost function parameter.

The designed control is subsequently tested on the a priori prepared datasets and the results analysed by several evaluation metrics examining different aspects of the control, such as BESS utilization in equivalent full battery cycles or energy exchange with the main grid.

The evaluated results clearly show that the proposed algorithm reacts to the changes of its control parameters. Different parameter settings were tested by simulations on independent datasets from time intervals of 3 weeks and the most convenient parameter set was found.

Finally, the control with the optimal parameter set is applied to the whole dataset. Also, this finally selected test reveals relative system cost reduction of up to approximately 6% compared to the reference control mechanism.

From the provided simulation several dependencies are observable. Firstly, the control parameter Q which sets the emphasis on the BESS SoC changes the utilization of the battery pack significantly. The same effect is observed during the extension of the control parameter predictive horizon. Therefore, the changes of these parameters can be used when the BESS is not utilized adequately.

The second important conclusion of the simulation results is the dependency of the relative cost reduction on the difference of absolute values of energy supplied and drawn from the main grid. When the total algebraic sum of the energy exchange is low, the algorithm proves to be more profitable.

This feature of the control algorithm can be explained by the general control idea. The MPC controller is trying to postpone the purchase or sale of energy from the main grid according to global price data with the utilization of the BESS. In case of a large difference between absolute values of $E_{tot,in}$ and $E_{tot,out}$, the algorithm has a limited range and the algorithm's profitability is decreasing.

There are several possibilities to improve the suggested control algorithm in future work. The consensus algorithm suffers from the requirement to set initial conditions for iteration. One possible approach to improve the algorithm is to iteratively search for the optimal initial conditions depending on power deficit or surplus of individual agents. Adjusting all agent's initial consensus values, the optimal final consensus value could be found and the necessary communication could be reduced.

Another suggested improvement of the algorithm is the adaptation of the BESS ageing process into the MPC objective function to minimize system cost. Li-ion batteries ageing is a very complex process depending on many factors such as charging and discharging currents, depth of discharge, median of BESS SoC or the temperature of the pack. With the careful extension of the cost function to include these factors, an optimal process considering the batteries ageing could be reached.

In general, the results of the proposed control architecture appear to be very promising. The designed algorithm can create a notable cost reduction which proves to be a strong argument for its selection for any future microgrid solution.

However, the implementation would require an existing communication infrastructure to enable multi-agent consensus. Thus, future work could also focus on determining a trade-off between communication extension to unfold advanced control mechanisms, in comparison to a reference control scheme with no communication.

Bibliography

[1] P. Elis et al. "Multi-agent MPC protocol for microgrid energy management and optimization". Submitted for consideration on IFAC conference, Berlin 2020.

[2] Nikos Hatziargyriou. *Microgrids: architectures and control.* John Wiley & Sons, 2014.

[3] Magdi S Mahmoud. *Microgrid: advanced control methods and renewable energy system integration.* Elsevier, 2016.

[4] T. L. Nguyen et al. "Agent based distributed control of islanded microgrid — Real-time cyber-physical implementation". In: *2017 IEEE PES Innovative Smart Grid Technologies Conference Europe (ISGT-Europe).* 2017, pp. 1–6. DOI: 10.1109/ISGTEurope.2017.8260275.

[5] T. Morstyn, B. Hredzak, and V. G. Agelidis. "Control Strategies for Microgrids With Distributed Energy Storage Systems: An Overview". In: *IEEE Transactions on Smart Grid* 9.4 (2018), pp. 3652–3666. ISSN: 1949-3053. DOI: 10.1109/TSG.2016.2637958.

[6] Reza Olfati-saber, J. Alex Fax, and Richard M. Murray. "Consensus and cooperation in networked multi-agent systems". In: *Proceedings of the IEEE.* 2007, p. 2007.

[7] M. I. Abouheaf and F. L. Lewis. "Multi-agent differential graphical games: Nash online adaptive learning solutions". In: *52nd IEEE Conference on Decision and Control.* 2013, pp. 5803–5809. DOI: 10.1109/CDC.2013.6760804.

[8] M. Reyasudin Basir Khan, Razali. Jidin, and Jagadeesh. Pasupuleti. "Multi-agent based distributed control architecture for microgrid energy management and optimization". In: *Energy Conversion and Management* 112 (2016), pp. 238–307.

[9] Y. Han et al. "MAS-Based Distributed Coordinated Control and Optimization in Microgrid and Microgrid Clusters: A Comprehensive Overview". In: *IEEE Transactions on Power Electronics* 33.8 (2018), pp. 6488–6508. ISSN: 0885-8993. DOI: 10.1109/TPEL.2017.2761438.

[10] J.M. Maciejowski. *Predictive Control with Constraints.* England.: Prentice Hall, 2002.

[11] John Rossiter. *Model-based Predictive Control-a Practical Approach.* Jan. 2003. DOI: 10.1201/9781315272610.

[12]   Y. Xue et al. "A comparison between two MPC algorithms for demand charge reduction in a real-world microgrid system". In: *2016 IEEE 43rd Photovoltaic Specialists Conference (PVSC)*. 2016, pp. 1875–1880. DOI: `10.1109/PVSC.2016.7749947`.

[13]   Alessandra Parisio, Evangelos Rikos, and Luigi Glielmo. "A Model Predictive Control Approach to Microgrid Operation Optimization". In: *Control Systems Technology, IEEE Transactions on* 22 (Sept. 2014), pp. 1813–1827. DOI: `10.1109/TCST.2013.2295737`.

[14]   Alessandra Parisio et al. "Use of model predictive control for experimental microgrid optimization". In: *Applied Energy* 115 (Feb. 2014), 37–46. DOI: `10.1016/j.apenergy.2013.10.027`.

[15]   G. Gürses-Tran et al. "MPC based energy management optimization for a european microgrid implementation". In: *25th International Conference on Electricity Distribution*. Vol. Paper 1908. 2019.

[16]   Y. Xu and Z. Li. "Distributed Optimal Resource Management Based on the Consensus Algorithm in a Microgrid". In: *IEEE Transactions on Industrial Electronics* 62.4 (2015), pp. 2584–2592. ISSN: 0278-0046. DOI: `10.1109/TIE.2014.2356171`.

[17]   S. Luo et al. "Multi-agent systems using model predictive control for coordinative optimization control of microgrid". In: *2017 20th International Conference on Electrical Machines and Systems (ICEMS)*. 2017, pp. 1–5. DOI: `10.1109/ICEMS.2017.8056293`.

[18]   Z. Guoping, W. Weijun, and M. Longbo. "An Overview of Microgrid Planning and Design Method". In: *2018 IEEE 3rd Advanced Information Technology, Electronic and Automation Control Conference (IAEAC)*. 2018, pp. 326–329. DOI: `10.1109/IAEAC.2018.8577763`.

[19]   R. Venkatraman and S. K. Khaitan. "A survey of techniques for designing and managing microgrids". In: *2015 IEEE Power Energy Society General Meeting*. 2015, pp. 1–5. DOI: `10.1109/PESGM.2015.7286590`.

[20]   R. Lasseter *et al.* "Integration of Distribution Energy Resources - The CERTs Microgrid concept". In: *Consortium for Electric Reliability Technology Solutions* (2002).

[21]   L. Tao et al. "From laboratory Microgrid to real markets — Challenges and opportunities". In: *8th International Conference on Power Electronics - ECCE Asia*. 2011, pp. 264–271. DOI: `10.1109/ICPE.2011.5944600`.

[22]   "IEEE Standard for the Specification of Microgrid Controllers". In: *IEEE Std 2030.7-2017* (2018), pp. 1–43.

[23]   F. Katiraei, M. R. Iravani, and P. W. Lehn. "Micro-grid autonomous operation during and subsequent to islanding process". In: *IEEE Transactions on Power Delivery* 20.1 (2005), pp. 248–257. ISSN: 0885-8977. DOI: `10.1109/TPWRD.2004.835051`.

[24] Xiong Liu, Peng Wang, and Poh Chiang Loh. "A hybrid AC/DC micro-grid". In: *2010 Conference Proceedings IPEC*. 2010, pp. 746–751. DOI: 10.1109/IPECON.2010.5697024.

[25] B. Kroposki et al. "Microgrids: Technologies and Testing". In: *IEEE Power and Energy Magazine* (2008).

[26] I. Erlich, M. Wilch, and C. Feltes. "Reactive power generation by DFIG based wind farms with AC grid connection". In: *2007 European Conference on Power Electronics and Applications*. 2007, pp. 1–10. DOI: 10.1109/EPE.2007.4417777.

[27] S. Zhou. "Study of Control and Efficiency of AC-DC Converter". In: *2010 International Conference on Electrical and Control Engineering*. 2010, pp. 4250–4253. DOI: 10.1109/iCECE.2010.1033.

[28] V. V. Joshi, N. Mishra, and D. Malviya. "A Vector Control Based Supercapacitor Current Control Algorithm for Fuel Cell and Battery - Supercapacitor Integrated Electric Vehicles". In: *2018 IEEE 8th Power India International Conference (PIICON)*. 2018, pp. 1–6. DOI: 10.1109/POWERI.2018.8704381.

[29] A. M. S. Yunus and M. Saini. "Overview of SMES units application on smart grid systems". In: *2016 International Seminar on Intelligent Technology and Its Applications (ISITIA)*. 2016, pp. 465–470. DOI: 10.1109/ISITIA.2016.7828705.

[30] R. Majumder. "Some Aspects of Stability in Microgrids". In: *IEEE Transactions on Power Systems* 28.3 (2013), pp. 3243–3252. ISSN: 0885-8950. DOI: 10.1109/TPWRS.2012.2234146.

[31] Mariya Soshinskaya et al. "Microgrids: Experiences, barriers and success factors". In: *Renewable and Sustainable Energy Reviews* 40 (2014), pp. 659 – 672. ISSN: 1364-0321. DOI: https://doi.org/10.1016/j.rser.2014.07.198. URL: http://www.sciencedirect.com/science/article/pii/S1364032114006583.

[32] Carmen Wouters. "Towards a regulatory framework for microgrids—The Singapore experience". In: *Sustainable Cities and Society* 15 (2015), pp. 22 – 32. ISSN: 2210-6707. DOI: https://doi.org/10.1016/j.scs.2014.10.007. URL: http://www.sciencedirect.com/science/article/pii/S2210670714001152.

[33] Hassan Harb. "Predictive Demand Side Management Strategies for Residential Building Energy Systems". PhD thesis. E.ON Energy Research Center, RWTH Aachen University, 2017.

[34] A. Monti et al. *Dual Demand SideManagement*. Tech. rep. Project No. 30. Institute for Automation of Complex Power Systems, Institute for Energy Efficient Buildings, and Indoor Climate, 2014, p. 150.

[35] Lokeshgupta Bhamidi, Arindam Sadhukhan, and S. Sivasubramani. "Multi-objective optimization for demand side management in a smart grid environment". In: Dec. 2017, pp. 200–205. DOI: 10.1109/ICPES.2017.8387293.

[36] Jingshuang Shen, Chuamwen Jiang, and Bosong Li. "Controllable Load Management Approaches in Smart Grids". In: *Energy Conservation in Infrastructures* (2015). ISSN: 1996-1073.

[37] A. Bidram, A. Davoudi, and F. L. Lewis. "A Multiobjective Distributed Control Framework for Islanded AC Microgrids". In: *IEEE Transactions on Industrial Informatics* 10.3 (2014), pp. 1785–1798. ISSN: 1551-3203. DOI: 10.1109/TII.2014.2326917.

[38] J. Timmermans et al. "Batteries 2020 — Lithium-ion battery first and second life ageing, validated battery models, lifetime modelling and ageing assessment of thermal parameters". In: *2016 18th European Conference on Power Electronics and Applications (EPE'16 ECCE Europe)*. 2016, pp. 1–23. DOI: 10.1109/EPE.2016.7695698.

[39] A. Etxeberria et al. "Hybrid Energy Storage Systems for renewable Energy Sources Integration in microgrids: A review". In: *2010 Conference Proceedings IPEC*. 2010, pp. 532–537. DOI: 10.1109/IPECON.2010.5697053.

[40] Mohammed I. Abouheaf et al. "Multi-agent discrete-time graphical games and reinforcement learning solutions". In: *Automatica* 50.12 (2014), pp. 3038 –3053. ISSN: 0005-1098. DOI: https://doi.org/10.1016/j.automatica.2014.10.047. URL: http://www.sciencedirect.com/science/article/pii/S0005109814004282.

[41] Y. Cao et al. "An Overview of Recent Progress in the Study of Distributed Multi-Agent Coordination". In: *IEEE Transactions on Industrial Informatics* 9.1 (2013), pp. 427–438. ISSN: 1551-3203. DOI: 10.1109/TII.2012.2219061.

[42] Y. Xu and W. Liu. "Novel Multiagent Based Load Restoration Algorithm for Microgrids". In: *IEEE Transactions on Smart Grid* 2.1 (2011), pp. 152–161. ISSN: 1949-3053. DOI: 10.1109/TSG.2010.2099675.

[43] J. B. Rawlings. "Tutorial overview of model predictive control". In: *IEEE Control Systems Magazine* 20.3 (2000), pp. 38–52. ISSN: 1066-033X. DOI: 10.1109/37.845037.

[44] Carlos E. García, David M. Prett, and Manfred Morari. "Model predictive control: Theory and practice—A survey". In: *Automatica* 25.3 (1989), pp. 335 –348. ISSN: 0005-1098. DOI: https://doi.org/10.1016/0005-1098(89)90002-2. URL: http://www.sciencedirect.com/science/article/pii/0005109889900022.

[45] S. Shariati and D. Abel. "Model Predictive Control in two days: Educating a new way of thinking". In: *IFAC-PapersOnLine* 49.6 (2016). 11th IFAC Symposium on Advances in Control Education ACE 2016, pp. 40 –45. ISSN: 2405-8963. DOI: `https://doi.org/10.1016/j.ifacol.2016.07.150`. URL: `http://www.sciencedirect.com/science/article/pii/S240589631630355X`.

[46] *MathWorks Matlab function fillmissing.* `https://de.mathworks.com/help/matlab/ref/fillmissing.html?searchHighlight=fillmissing&s_tid=doc_srchtitle`.

[47] *Nord Pool group Day-ahead prices.* `http://https://www.nordpoolgroup.com/Market-data1/Dayahead/Area-Prices/SE/Hourly/?dd=SE4&view=table`.

[48] *Statista Average prices of diesel fuel in Sweden from 2000 to 2018 (in euros).* `https://www.statista.com/statistics/603731/diesel-fuel-prices-sweden/`.

[49] *Diesel generators Approximate Diesel Fuel Consumption Chart.* `https://www.dieselgenerators.com/approximate-diesel-fuel-consumption-chart`.

[50] *MathWorks Matlab function arima.* `https://de.mathworks.com/help/econ/arima.html`.

List of Figures

List of Tables

Appendix

A Content of the attached CD

1. Literature - A folder containing all the utilized literature

2. Matlab - A folder containing the whole used Matlab program

3. Multi-agent MPC protocols for microgrid energy management and optimization.pdf